NACA RM A8L28

Copy No.

[redacted]

RM No. A8L28

UNCLASSIFIED

NACA RM No. A8L28

NACA

CASE FILE
COPY

RESEARCH MEMORANDUM

HEAT-TRANSFER AND BOUNDARY-LAYER TRANSITION ON A HEATED 20° CONE AT A MACH NUMBER OF 1.53

By Richard Scherrer, William R. Wimbrow,
and Forrest E. Gowen

Ames Aeronautical Laboratory
Moffett Field, Calif.

Classification Changed to
By
Date

JPL LIBRARY
CALIFORNIA INSTITUTE OF TECHNOLOGY

CLASSIFIED DOCUMENT

This document contains classified information affecting the National Defense of the United States within the meaning of the Espionage Act, USC 50:31 and 32. Its transmission or the revelation of its contents in any manner to an unauthorized person is prohibited by law. Information so classified may be imparted only to persons in the military and naval services of the United States, appropriate civilian officers and employees of the Federal Government who have a legitimate interest therein, and to United States citizens of known loyalty and discretion who of necessity must be informed thereof.

NATIONAL ADVISORY COMMITTEE
FOR AERONAUTICS

WASHINGTON
January 10, 1949

UNCLASSIFIED

[redacted]

DEC 7 0 1949

UNCLASSIFIED
Unclassified

 [redacted]

NATIONAL ADVISORY COMMITTEE FOR AERONAUTICS

RESEARCH MEMORANDUM

HEAT-TRANSFER AND BOUNDARY-LAYER TRANSITION ON A HEATED 20° CONE AT A MACH NUMBER OF 1.53

By Richard Scherrer, William R. Wimbrow, and
Forrest E. Gowen

SUMMARY

Heat-transfer data from supersonic wind-tunnel tests of a heated 20° cone have been compared with theoretical results obtained by two methods for determining the convective heat transfer in laminar boundary layers in a compressible fluid. The cone was heated electrically and was tested at a Mach number of 1.53. Local rate of heat transfer and surface-temperature measurements were made over a range of Reynolds numbers and nominal surface temperatures with both laminar and turbulent boundary layers.

The theoretical and experimental results in the case of the laminar boundary layer were found to be in good agreement in terms of the heat-transfer coefficients in the region on the test body where the theory was considered applicable. Good agreement in terms of rate of heat transfer was obtained by the use of the theoretical heat-transfer coefficients and the true temperature potential. The effect of heat transfer on boundary-layer stability was indicated by surface-temperature measurements for a uniform power input distribution, the sudden decrease in surface temperature at the beginning of the turbulent boundary-layer region being indicative of the transition. The results provided a qualitative verification of the effect of heat transfer on laminar boundary-layer stability that had been predicted theoretically by Lees. (NACA Technical Note No. 1360.)

The general heat-transfer equations developed in NACA TN No. 1300 are shown to reduce, for cones, to simple relationships,

[redacted]

Unclassified
UNCLASSIFIED

and these are presented in the form of design charts by which the local rate of heat transfer may be determined on cones with attached bow waves.

INTRODUCTION

Because of aerodynamic heating, the practical operation of aircraft at high speeds is dependent on the provision of adequate insulation and cooling systems for the aircraft structure, equipment, pay load, and occupants. The design of such systems, in turn, is dependent on the existence of adequate heat-transfer data and on the development of theories by which the data may be correlated and its application extended.

The most extensive experimental investigation to date in the field of heat transfer at high velocities was conducted in Germany by Eber. (See reference 1.) This work provides the basis for most heat-transfer calculations for proposed supersonic aircraft. However, the air flow in the test section of the supersonic wind tunnel at Kochel, in which Eber performed his experiments, was such that there has been some question as to the extent of the laminar boundary layer on the test bodies. (See fig. 5 of reference 1.) Since there are large differences in the rates of heat transfer through laminar and turbulent boundary layers, additional experiments have been needed to clarify Eber's results.

Another aspect of the heat-transfer problem, both at subsonic and supersonic speeds, is the effect of heat transfer on the stability of a laminar boundary layer. The theoretical work of Lees (reference 2) indicates that the effect of surface heating is destabilizing to a laminar boundary layer and also indicates that the effect of surface cooling is stabilizing. The results presented in reference 3 for a very low Mach number are in agreement with the results of reference 2; however, no experimental data are available to indicate the effect of heat transfer on boundary-layer stability at supersonic speeds.

The purpose of the investigation presented in this report was to obtain heat-transfer data on a body of revolution with first, a laminar boundary layer and, then, a turbulent boundary layer, and to compare

UNCLASSIFIED

these data with the theoretical results calculated by the methods of references 4 and 5 and with the results obtained by Eber. The qualitative effect of heat transfer on the stability of the laminar boundary was also to be determined.

SYMBOLS

The following symbols have been used in the presentation of the theoretical and experimental data:

A area, square feet

a speed of sound, feet per second

c_p specific heat at constant pressure, Btu per pound, $^{\circ}F$

c_v specific heat at constant volume, Btu per pound, $^{\circ}F$

c arbitrary constant

g gravitational constant, 32.2 feet per second squared

H total pressure, pounds per square foot, absolute

h local heat-transfer coefficient, Btu per hour, square foot, $^{\circ}F$

$\bar{h}$ average heat-transfer coefficient, Btu per hour, square foot, $^{\circ}F$

k thermal conductivity, Btu per hour, square foot, $^{\circ}F$ per foot

l body length, feet

M Mach number, dimensionless

m Mach number parameter $\left(\frac{\gamma-1}{2} M_v^2\right)$, dimensionless

$\overline{Nu}$ average Nusselt number $\left(\frac{\bar{h}s}{k_s}\right)$, dimensionless

Nu local Nusselt number $\left(\frac{hs}{k_s}\right)$, dimensionless

Nu_δ boundary-layer Nusselt number $\left(\frac{h\delta}{k_s}\right)$, dimensionless

Pr Prandtl number $\left(\frac{c_p\mu}{k} \times 3600g\right)$, dimensionless

[redacted]

p static pressure, pounds per square foot, absolute

[redacted]

UNCLASSIFIED

Q total rate of heat transfer, Btu per hour

q local rate of heat transfer, Btu per hour, square foot

R gas constant for air, 1718 foot squared per second squared, $^{\circ}F$

Re Reynolds number $\left(\frac{\rho_V V s}{\mu_s}\right)$, dimensionless

r radius of body, feet

s distance from nose along surface of the body, feet

T temperature, $^{\circ}F$ absolute

T_R recovery surface temperature, $^{\circ}F$ absolute

T_s' pseudo-surface temperature $[T_s' = \beta (T_o - T_v) + T_v]$, $^{\circ}F$ absolute

u fluid velocity parallel to the surface at any point within the boundary layer, feet per second

V fluid velocity just outside the boundary layer, feet per second

y distance normal to the body surface, feet

β surface-temperature parameter; for a Prandtl number of 1.0, $\beta = \left(\frac{T_s' - T_v}{T_o - T_v}\right)$ and for a Prandtl number of 0.73, $\beta = \left(\frac{T_s - T_v}{T_R - T_v}\right)$, dimensionless

γ ratio of specific heats (c_p/c_v), dimensionless

δ boundary-layer thickness, feet

θ_c cone half-angle, degrees

μ absolute viscosity, pound-second per square foot

ρ air density, slugs per cubic foot

σ^* air density ratio (ρ/ρ_a), dimensionless

τ unit surface shear, pounds per square foot

[redacted]

UNCLASSIFIED

In addition, the following subscripts have been used:

a reference air density

s fluid conditions at the body surface

v any point along the body, just outside the boundary layer

x location of a particular limit of integration along the length of the body

o fluid conditions at total temperature and pressure (after isentropic compression from static conditions)

1 fluid conditions just behind an attached oblique shock wave from the nose of a body

The superscript ' together with the subscript s have been used to indicate the pseudo-surface temperature, T_s', and the physical constants of air based on this temperature, μ_s' and k_s'.

ANALYSIS

In order to obtain continuity in this report, the various theoretical developments involved in the presentation and explanation of the test data are presented separately in appendices. Only the results of each development are presented in the text.

A method for calculating the rate of heat transfer in the laminar boundary-layer region of bodies of revolution in steady supersonic flight is presented in reference 4 and is used as the basis of the theoretical calculations for the present investigation. The method assumes a linear velocity profile within the laminar boundary layer and also assumes a Prandtl number of one, but considers the effect of compressibility. The general equations of reference 4 are shown in appendix A to reduce, for cones, to the single equation,

$$Nu = \frac{hs}{k_s'} = 1.225 \sqrt{B\ Re} \qquad (A15)^1$$

The equation defining the variable B, as a function of Mach number

[1]The equation designation (A15) indicates equation (15) of appendix A. This method of designation is used throughout this report.

[redacted]

UNCLASSIFIED

and surface-temperature parameter, is given in appendix A.

Equation (A15) gives the value of local Nusselt number or local heat-transfer coefficient at any point on a cone. However, in many heat-transfer problems the average heat-transfer coefficient is required rather than the local value. The average value of heat-transfer coefficient from the nose to any point on a cone with a laminar boundary layer is shown in appendix B to be given by the relation.

$$\bar{h} = \frac{4}{3} h \tag{B5}$$

This simple relationship, first recognized by Hantzsche and Wendt (reference 5) results from the form of equation (A15) and the geometry of cones. This equation may be used to convert local values of Nusselt number to average values as long as the surface temperature is constant.

In a laminar boundary layer in subsonic flow, the velocity profile is known to be very similar to the profile calculated by Blasius. Velocity profiles in a laminar boundary layer in supersonic air flow have not been measured for any appreciable range of Mach numbers, but the profiles have been calculated by several investigators. The trend of the calculated profile shapes with increasing Mach number is from the Blasius profile at subsonic Mach numbers toward an almost linear profile at a Mach number of 10. (See reference 6.) The effect of surface cooling at any Mach number is to make the velocity profile approach that of some lower Mach number, or to become less linear. Although a linear velocity profile is assumed in the development of the method of reference 4, the effect of this assumption is shown by the comparison between the methods of references 4 and 7 developed in appendix C. The method of reference 7 assumes a Blasius velocity profile in an incompressible fluid and assumes a Prandtl number of one. Since the only differences in the two methods are the profile assumptions and the consideration of compressibility in the method of reference 4, the difference in the results obtained by the two methods at some subsonic Mach number, at which compressibility can be neglected, would only be due to the velocity profile assumptions. In the comparison of the heat-transfer coefficients on a flat plate, given by the two methods, the method of reference 7 gives the relation

$$h = 0.332\ k \sqrt{\frac{Re}{s^2}} \tag{C5}$$

and from the method of reference 4, for M=0 and β=1.0,

[redacted]

UNCLASSIFIED

$$h = 0.286\ k \sqrt{\frac{Re}{s^2}} \tag{C7}$$

It is evident from the constants in the above equations that the effect of the linear velocity profile assumption, at the conditions of zero Mach number and zero heat transfer, is to decrease the calculated heat-transfer coefficient by about 15 percent relative to that obtained by the method of reference 7. The assumption of a linear velocity profile leads to a calculated boundary-layer thickness that is 50 percent greater than is the case with the method of reference 7 and a boundary-layer Nusselt number that is 30 percent greater. These two effects are partially compensating and the difference in the heat-transfer coefficients, as indicated by the constants in equations (C5) and (C7), is relatively small.

The local values of Nusselt number on cones with attached bow waves can be calculated by equation (A15) if the conditions of the air stream just outside the boundary layer are known. The details of the method by which the theoretical data based on reference 4 were calculated for this report are presented in appendix D together with a step-by-step outline of the method for using a series of design charts based on equation (A15).

APPARATUS AND TEST PROCEDURES

Wind Tunnel

The tests were performed in the Ames 1- by 3-foot supersonic wind tunnel No.1. This tunnel was temporarily equipped with a 1- by 2-1/2-foot test section and a fixed nozzle that provided a test-section Mach number of 1.53. Since no aerodynamic forces were to be measured, the strain-gage balance equipment was removed and the test cone was mounted with a suitable adapter to the balance housing.

Test Cone

The usual case of heat transfer at supersonic speeds is for heat to flow into the surface rather than out of the surface. From the theoretical aspect either case would be satisfactory to obtain a partial check on the theory of reference 4, but a complete comparison requires the testing of both a heated and a cooled body under similar test conditions. An electrically heated cone was chosen for these tests because of the simplicity of the experimental techniques which could be employed.

[redacted]

UNCLASSIFIED

The 20° cone was constructed as shown in figure 1. The exterior shell was machined from stainless steel and all other metal parts were made of copper. The exterior surface of the model had a smooth, ground finish, estimated to be a 30-microinch root mean square (rms) surface. The walls of the shell were tapered to maintain an approximately constant incremental resistance along the cone length when cold. The cone was heated by passing a high amperage (800 amperes maximum), low voltage (0.45 volts maximum), alternating electrical current longitudinally through the cone surface. Because no current would flow through the extreme nose of the cone, the forward 25 percent of the cone was in effect unheated.

Eight thermocouples were installed at equal length increments along the cone to allow determination of the temperature distribution. The thermocouples were made from 30-gage copper-constantan duplex wire with welded junctions. They were installed in holes drilled completely through the shell and were soldered in place. Ten leads of 20-gage copper wire were also installed in the shell, in a similar manner, to provide a means of measuring incremental voltage drops along the cone. The locations of the thermocouples and the voltage leads are indicated in figure 1. A photograph of the assembled cone is shown in figure 2, and a photograph of the cone installed in the wind tunnel is shown in figure 3.

Instrumentation

The wiring of the test cone was connected as shown in figure 4. The variable voltage transformer controlled the input to the primary side of the power transformer. The secondary side of the power transformer was grounded to the tunnel shell which acted as one lead in the circuit. The other lead consisted of two parallel cables that were connected to two binding posts at the base of the cone. Two cables were used to keep the cable size down to a convenient diameter. These cables passed through a current transformer which was in turn connected to an ammeter to measure the current input to the cone.

The eight thermocouples were connected through a selector switch to a potentiometer. The potentiometer was used to obtain a zero reading on an external light-beam galvanometer, the potentiometer output then being equal to the thermocouple potential.

The ten voltage leads from the cone were connected through a selector switch to an electronic voltmeter in such a manner as to measure the voltage drops of successive increments along the cone. The local power input, or rate of heat transfer per unit length,

is given by the product of the current and the incremental voltage drop.

The total temperature of the air stream was measured by nine thermocouples in the tunnel settling chamber which were connected through a selector switch to a direct reading potentiometer.

Procedure

Data were obtained over a range of Reynolds numbers from approximately 0.5 to 2.5 millions. This variation of Reynolds number was effected by varying the pressure level within the tunnel. The tunnel was first brought to the desired pressure and then allowed to run until the general temperature distribution on the cone came to equilibrium. When this condition was reached, the surface temperature of the cone was measured by the surface thermocouples. The surface temperature measured under these conditions (zero heat flow) is called the recovery surface temperature, or just recovery temperature T_R. The heating circuit was then closed and the cone heated to the desired temperature, as indicated by the potentiometer reading of the most forward surface thermocouple, by adjusting the input voltage. Since the average total temperature of the air stream was in the order of 100° F, cone temperatures of 120°, 140°, 160°, 180°, and 200° F were arbitrarily chosen as nominal values at which to obtain data. The surface temperature varied along the length of the cone through a range of about 5° to 35°, depending on the temperature level, the front of the heated section of the cone always being the hottest.

With the cone at the desired temperature, the following data were read and recorded: the total pressure and total temperature of the air stream, the current input to the cone, the incremental voltage drops, and the local surface temperatures of the cone. These data were obtained at each of the nominal cone temperatures previously mentioned and at nominal values of total pressure of 3, 6, 9, 15, and 21 pounds per square inch absolute.

Upon completion of the tests described, surface roughness was employed to obtain data with a completely turbulent boundary layer. Approximately the first 2 inches of the nose of the cone were sprayed with clear lacquer and, before the lacquer was completely dry, it was sprayed again with lampblack in suspension in lacquer thinner. After the thinner evaporated, the lampblack adhered to the lacquer base and provided a band of fairly uniform roughness around the nose of the cone. Liquid-film tests were performed to determine if the roughness was sufficient to cause premature transition. It was found that at

total pressures above 6 pounds per square inch absolute, the boundary layer was completely turbulent. Tests similar to those previously described were performed at nominal total pressures of 9 and 15 pounds per square inch absolute with the completely turbulent boundary layer.

ACCURACY OF RESULTS

The accuracy of the experimental data was determined by estimating the uncertainty of the individual measurements which entered into the determination of the final results. The over-all uncertainty of any given parameter was then obtained by geometric summation of the uncertainty of each of the factors entering the final value of that parameter as indicated by the method employed in reference 8.

The estimated uncertainty of the basic measurements are as follows:

Total temperature . . . . . $T_o \pm 2^\circ$ F

Recovery surface temperature . . . . . $T_R \pm 0.5^\circ$ F

Free-stream temperature just outside the boundary layer . $T_v \pm 2^\circ$ F

Surface temperature . . . . . $T_s \pm 0.5^\circ$ F

Total pressure . . . . . $H_o \pm 0.05$ centimeters of mercury

Incremental voltage drops . . . . . $\Delta E \pm 2$ percent

Input amperage . . . . . $I \pm 8$ amperes (1 to 3 percent)

Cone dimensions . . . . . ± 0.005 inch

Cone segment surface areas . . . . . ± 3.2 percent

The calculated accuracy of the final parameters are as follows:

Surface-temperature parameter . . . . . $\beta \pm 2.4$ percent

Temperature potential . . . . . $\Delta T \pm 4.3$ percent at $\beta=1.4$
± 1.5 percent at $\beta=2.0$

Local rate of heat transfer, ... $q \pm 4.1$ to ± 5.0 percent

Heat-transfer coefficient . . . . . .h ±4.4 to ±6.6 percent

Nusselt number . . . . . Nu ±4.4 to ±6.6 percent

Reynolds number . . . . . Re ±1.8 to ±1.9 percent

A further error was introduced in the experimental data by radiation of heat energy from the cone to the tunnel walls and an effort was made to determine the order of magnitude of the radiation by experimental means. The total heat transferred from the cone is equal to the sum of the convective and radiant heat transfer plus the end losses, and the radiant heat transfer is proportional to the difference in the fourth powers of the absolute temperatures of the cone and wind-tunnel wall. The convective heat transfer is a function of total pressure and will become zero when the total pressure is reduced to zero. Therefore, at zero total pressure, the heat transfer will be entirely due to radiation. Since it is impossible to evacuate the tunnel to zero pressure and measure the heat transferred by radiation directly, the heat loss due to radiation was evaluated from the data obtained at the various test conditions with the tunnel in operation.[2]

The total heat transferred Q as measured at the various pressures was divided by the difference in the fourth powers of the cone and tunnel-wall absolute temperatures, and the resulting parameter $\frac{Q}{T_s^4-T_w^4}$ was plotted logarithmically against the corresponding total pressures. Because the surface temperatures along the cone were not equal, data obtained by cross-plotting was used in the determination of the correction for radiant heat transfer.[3] The ordinate of the logarithmic plot at zero pressure is a measure of the heat transferred to the tunnel walls by radiation and includes such factors as the Stephan-Boltzman constant, the shape factor, and the emissivities of the cone and walls. The quantity thus attained, however, was so small as to be completely masked in the ±5-percent uncertainty of the measured heat transfer. Solutions for several of the elements gave slightly negative losses. Consequently, the correction for radiation was assumed to be negligible.

---

[2]An attempt was made to obtain the radiation calibration with the tunnel inoperative, but the cone surface temperatures were found to be very erratic because of free-convection currents. For this reason the method was abandoned.

[3]The method of reducing the data to constant values of surface-temperature parameter is discussed in detail in the section of this report titled "Results and Discussion."

Conduction along the skin of the cone also affected the data at the base and at the nose. Calculations show that about 10 percent of the total heat generated in the first heated element is conducted to the unheated nose portion and a slightly higher percentage is lost from the last element through the base of the cone. Data from the first and last elements have been neglected in the analysis of the test data and the elements between these two appear to receive as much heat from neighboring elements as they lose. Consequently, the conduction losses are assumed to be negligible. The test Mach number, 1.53, was selected as the average of the linear Mach number gradient in the region in which the model was installed and the maximum deviation from the average Mach number was approximately ± 0.02. The Mach number gradient in the test section was neglected in the reduction of the test data.

RESULTS AND DISCUSSION

The measurements of local power input were converted to local rates of heat transfer by dividing by the incremental areas and converting the electrical units to heat units. Heat-transfer coefficients were obtained from the local rates of heat transfer by dividing by the temperature potential $(T_S - T_R)$. Nusselt numbers were obtained by the combination of the appropriate values of heat-transfer coefficient, reference length, and thermal conductivity as previously defined.

Laminar Boundary-Layer Heat Transfer

The surface-temperature distributions along the cone for various nominal values of surface temperature are shown in figure 5. The temperature variation with length is due to the local values of electrical resistance and the heat-transfer-coefficient distribution. The heat-transfer rates in a turbulent boundary layer are, in general, much greater than those in a laminar boundary layer; therefore, the sudden drop in surface temperature toward the base of the cone, which appears in figures 5(d) and 5(e), is indicative of transition to turbulent flow within the boundary layer.

A rigorous comparison of theory and experiment would require constant values of surface-temperature parameter and hence constant surface temperature along the length of the cone. However, the surface

temperatures obtained in the experiments were not constant. In order to make the desired comparison, the original data were plotted as local heat-transfer rate as a function surface-temperature parameter, as shown in figure 6. Lines for each longitudinal segment of the cone were drawn through the data points. The values of local heat-transfer rate for constant values of surface-temperature parameter were then obtained by cross-plotting.

The comparison of the data, on the basis of constant values of surface-temperature parameter with a changing surface temperature, involves the assumption that the small variation in surface temperature ahead of a particular point on the cone does not affect the heat transfer at that point. The validity of this assumption is illustrated in figure 7 by a comparison of data for a nominal surface temperature of 180° F and cross-plotted data for a surface-temperature parameter of 1.8 on the basis of the Nusselt number - Reynolds number relationship. The lines in figure 7 are faired through the data obtained on the aft portion of the cone only. The difference between the two methods of data presentation is small, and for this reason the comparison of theory and experiment in terms of constant values of surface-temperature parameter is valid for the present experiments. It should be noted that the cross-plotted data are indicated by flagged symbols. This method of indicating cross-plotted data has been used throughout this report.

The effect of the large variation in surface temperature which occurs at the beginning of the heated portion of the cone $(s/l=0.25)$ is indicated by the initially decreasing values of Nusselt number with increasing Reynolds number for each tunnel pressure. (See fig. 7.) This effect can be explained by consideration of the changes which occur in the boundary-layer temperature profile as the layer flows along the cone.

The local rate of heat transfer at any point on the cone is given by the product of the thermal conductivity of the air adjacent to the surface and the slope of the boundary-layer-temperature profile at the surface. At the beginning of the heated portion of the test cone, a relatively cold boundary layer flows onto the heated area and the slope of the boundary-layer-temperature profile becomes large because of the large difference between the air and surface temperatures. The air temperature at the surface will approach the surface temperature as the air continues to flow along the heated surface, or the local rate of heat transfer downstream of the surface-temperature discontinuity will approach the value that would have existed if the surface-temperature discontinuity had not been present. The data shown in figure 7

indicate this tendency toward the rear of the cone where the change in surface temperature with length is small in comparison with that near the nose.

The effect of heating the aft portion of the cone will be to increase the boundary-layer thickness in this region. The resulting laminar boundary-layer thickness can be calculated, at least approximately, by the following method: If the surface temperature is assumed to be discontinuous at the edge of the heated region (no longitudinal conduction), the boundary-layer thickness at any point on the cone, either heated or unheated over its entire length, can be calculated by the method of reference 4. The boundary-layer thickness at any point along the heated portion can be approximated (as shown in fig.8) as the thickness of the boundary layer for a completely heated cone less the difference in boundary-layer thicknesses at the edge of the heated portion, for a completely heated cone and for an unheated cone. The correction obtained by this method is small at the beginning of the heated region on the cone, and, because the correction is small, it can be expected to be reasonably accurate at any downstream position. At some point far downstream, where the boundary-layer thickness is considerably greater than at the beginning of the heated region, the percent error in boundary-layer thickness would be insignificant.

A comparison of the theoretical local heat-transfer coefficients for the heated- and unheated-nose conditions with the experimental values for a surface-temperature parameter of 1.4 is shown in figure 9. The agreement between the experimental and the theoretical values, corrected for the effect of the unheated nose, is good over the after portion of the cone. Figure 9 also indicates the failure of any method for calculating heat-transfer coefficients, based on boundary-layer thickness, when a large change occurs in the assumed relation between the boundary-layer velocity profile and temperature profile. A method based on different assumptions is needed to calculate the local rates of heat transfer in regions where large surface-temperature gradients exist. Such a method will be necessary in order to calculate the optimum location of surface-cooling heat exchangers for high-speed aircraft.

The experimental and theoretical values of local Nusselt number are shown as functions of length Reynolds number and surface-temperature parameter in figure 10. The theoretical values are corrected for the effect of the unheated nose by the method illustrated in figure 8. The effect of the correction is to alter the slope of the lines from the 2:1 slope indicated by equation (A15). The

correction also produces the discontinuities between the lines for each value of total pressure, because the value of boundary-layer thickness to which the Nusselt number is related is not directly related to the length Reynolds number for the different values of total pressure.

It should be noted in figure 10 that the agreement between slopes of the theoretical lines (reference 4) and the trend of the data is almost exact within the small scatter of the data. This agreement is indicative of the accuracy of correcting the boundary-layer thickness for the effect of the unheated nose, because the thickness correction primarily affects the exponent of the Nusselt number to Reynolds number relationship.

The relationship derived by Hantsche and Wendt (reference 5) for laminar boundary layers is also plotted in figure 10 for comparison with the experimental data and the comparable results calculated by the method of reference 4.

For a rigorous comparison of theory and experiment, the effect of each of the test conditions on the final results should be known. The following variables affect laminar boundary-layer thickness and therefore the heat transfer at any point on a test body:

1. Distance along the body

2. Velocity of air flow along the body

3. Ambient-air temperature

4. Surface temperature

5. Ambient-air pressure

6. Surface-pressure gradient

7. Surface-temperature gradient

8. Surface roughness

The effects of the first five of these variables are accounted for in equation (A15), and the effect of surface-pressure gradient has been eliminated from the experiments by the selection of a cone for a test body. However, a small pressure or Mach number gradient does exist in the wind-tunnel nozzle. An approximate correction

for the effect of surface-temperature gradient on boundary-layer thickness has been made in the comparison of theory with experiment. However, the effect of the surface-temperature gradient on the assumed boundary-layer temperature and velocity-profile relationship cannot be included in the correction. The effect of surface roughness on laminar boundary-layer thickness is not known quantitatively for the surface finish on the test cone. Since surface roughness will be present to some extent on all supersonic aircraft, its effects should be investigated, at least to the extent of determining a value of roughness below which there will be little or no effect on laminar-boundary-layer thickness or stability.

The agreement between the theoretical results based on references 4 and 5 and the experimental data, shown in figure 10, is satisfactory over the rear portion of the cone where the theories are considered to be applicable. Whether or not the comparison is favorably or adversely affected by surface roughness, pressure gradients or surface-temperature gradients can only be determined by fundamental investigations of each of these effects.

The plots of experimental local heat-transfer coefficient against surface-temperature parameters from which cross plots were made indicated a slight decrease in heat-transfer coefficient with reduction in surface-temperature parameter; however, this trend was within the range of the experimental accuracy (± 6 percent) as is the trend indicated by the theory of reference 4 (± 4 percent). For this reason, the heat-transfer-coefficient distributions of figure 11 are shown as only functions of total pressure.

Satisfactory agreement between theory and experiment is shown in figure 11 over the rear portion of the cone where the theory is considered to be applicable. Because of this agreement, in terms of heat-transfer coefficient, poor agreement between the theory of reference 4 and experiment in terms of local rate of heat transfer can be expected because of the incorrect temperature potential in the theoretical equation $[q=h(T_s'-T_o)]$. Therefore, it appears logical to use the true temperature potential, corresponding to a Prandtl number of 0.73 (T_s-T_R) in the theoretical calculations of local rate of heat transfer rather than that corresponding to a Prandtl number of one $(T_s'-T_o)$ that a rigorous interpretation of the theory would dictate. The desirability of this empirical change in the theory is indicated by the more satisfactory agreement between theory and experiment shown by the curves for a Prandtl number of 0.73 in figure 12.

Laminar-Boundary-Layer Stability

The streamwise extent of the laminar boundary layer on the cone for various surface temperatures is indicative of the effect of heat transfer on boundary-layer stability. The distance from the nose of the test body to the transition point was obtained from the surface-temperature distribution curves of figure 5. The inflection points on the curves of figure 5, as indicated by the black dots, were selected as being the average transition points. The effect of heat transfer on boundary-layer stability is shown in figure 13 as a plot of the length Reynolds number at the transition point against the average surface-temperature parameter up to the indicated transition point. The decrease in transition Reynolds number with increasing surface-temperature parameter confirms the prediction of reference 2 and agrees with the experimental results of reference 3. The curve of figure 13 shows a hyperbola-like variation of the transition Reynolds number with surface-temperature parameter, indicating that the rate of change of boundary-layer stability $\left(\frac{\partial Re_t}{\partial \beta}\right)$ decreases with decreasing stability. The difference between the values of Reynolds number for transition at 15 and 21 pounds per square inch total pressure is believed to be due to a change in air-stream turbulence level.

Turbulent Boundary-Layer Heat Transfer

The experimental surface temperature and local rate of heat-transfer distributions along the 20° cone with an artificially induced turbulent boundary layer are shown in figures 14 and 15. The same data in the nondimensional form of local Nusselt number as a function of length Reynolds number are shown in figure 16. Because of the scatter, a line of 0.8 slope (the known slope for turbulent boundary layers) was faired through the data points. The points which are displaced farthest above the line are those from the forward portion of the cone and, as in the case of the laminar boundary-layer data, are affected by the surface-temperature discontinuity at the beginning of the heated region.

A comparison of the average values of Nusselt number from the turbulent boundary-layer data with the results obtained by Eber (reference 1), by Hantzsche and Wendt (reference 5), and those obtained for a laminar boundary layer from the design charts (appendix D) and corrected by the four-thirds factor to obtain average values of heat-transfer coefficient (appendix B) is made

in figure 17. The curves for each nominal value of surface temperature in figure 17 tend to approach a common line asymptotically. This result occurs because the percent effect of the large local Nusselt numbers in the nose region (due to the surface-temperature discontinuity) gradually decreases as more of the cone is included in the average. The asymptotes of the experimental lines were drawn with a slope of 0.8 which is also the slope of the line given by Eber's equation.

It is evident from a comparison of the various curves of figure 17 that Eber's results were obtained from test bodies with turbulent boundary layers. The low Reynolds numbers of Eber's tests should have produced laminar boundary layers; therefore, the transition must have been caused by external disturbances. Figure 5 of reference 1 shows the great number of shock waves which existed in the test section of the Kochel supersonic wind tunnel in which Eber conducted his experiments. It is known that such shock waves are very effective in causing premature transition of the laminar boundary layer. The fact that transition was induced artificially in both Eber's and the present experiments limits the applicability of the data. The difference between the turbulent boundary-layer data from the present experiments and the results given by Eber's equation is probably due to the difference in the methods of causing transition. In the present experiments transition was induced by roughness at the nose of the cone and the boundary layer was entirely turbulent. In Eber's experiments transition, due to shock waves, would be expected to occur farther aft on the cone and the boundary layer at the nose would be laminar. This being the case, the average heat-transfer coefficient and the average Nusselt number obtained by Eber should be lower than those obtained in the present experiments. The scatter of the data obtained by Eber would have masked any change in the slope of the Nusselt number – Reynolds number line that would be expected to result from mixed laminar and turbulent flow.

It follows from the preceding discussion that any turbulent boundary-layer heat-transfer data which are not obtained with natural transition or knowledge of the preceding laminar boundary layer will not be generally applicable to the calculation of the cooling requirements of supersonic aircraft. The fact that Eber's equation gives usable results when applied to the specific problem of calculating the temperature-time relationship of the skin at the nose of missiles indicates that turbulent boundary layers exist in this region or that the method of calculation rather than the data determines the results obtained.

If turbulent boundary layers do exist in the nose region of

missiles, improvements in shape and surface condition would allow longer runs of laminar boundary layer with the result that the rate of increase of surface temperature with time would be materially reduced. Also, the heat capacity or mass of the skin could be reduced for a given rate of increase of surface temperature. This latter effect would provide an improvement in mass ratio, and, therefore, an improvement in the range of the missile. The weight advantage of maintaining laminar boundary layers to reduce the required capacity of aircraft cooling systems would be apparent with any method of cooling.

CONCLUSIONS

The results of the foregoing investigation lead to the following conclusions:

1. Experimental heat-transfer coefficients obtained from tests of a heated 20° cone at a Mach number of 1.53 have been found to be in satisfactory agreement with two theoretical methods of calculating the rate of heat transfer in the laminar boundary-layer region of bodies of revolution in a compressible fluid.

2. Satisfactory agreement was obtained between the theoretical rates of heat transfer based on NACA TN No. 1300 and those determined by experiment, in the region of the test body where the theory is considered applicable, when the theoretical heat-transfer coefficients and the true temperature potential were employed.

3. The theoretical prediction of Lees (NACA TN No. 1360) that the effect of heating a surface with a laminar boundary layer to a temperature above the recovery surface temperature is to destabilize the boundary layer, has been confirmed experimentally at a Mach number of 1.53.

Ames Aeronautical Laboratory,
National Advisory Committee for Aeronautics,
Moffett Field, Calif.

[redacted]

[redacted]

APPENDIX A

LOCAL HEAT-TRANSFER COEFFICIENTS ON CONES

The general equation for laminar boundary-layer thickness on a body of revolution in a compressible fluid is, from reference 4,

$$\delta^2 = \frac{2C\left(\frac{l}{\sigma^*}\right)}{\left[\left(\frac{r}{l}\right)B\rho_V\right]_x^2}\int_0^{s_x/l}\left(\frac{r}{l}\right)^2 \frac{\rho_V\mu_s{}'B}{CV}\left(\frac{V}{V_x}\right)^{2\left(\frac{A}{B}\right)} d\left(\frac{s}{l}\right) \tag{A1}$$

in which

$$A = 1 + \frac{2}{m} + \frac{\beta-0.5}{m}\log_e(1+\beta m) + \frac{\beta(1-\beta)-Y^2}{2mY}\log_e Z$$

$$B = \frac{1}{m} + \frac{\beta}{2m}\log_e(1+\beta m) + \frac{1-\beta^2-Y^2}{4mY}\log_e Z$$

$$C = e^{2\int_{(A/B)_o}^{(A/B)_x}\log_e V\, d\left(\frac{A}{B}\right)}$$

$$Y = \left[\frac{4}{m}(1+\beta m) + (1-\beta)^2\right]^{1/2}$$

and

$$Z = \left[1 - \frac{2}{(1-\beta)-Y}\right]\left[\frac{(1-\beta)+Y}{(1-\beta)-2+Y}\right]$$

It should be noted that the physical properties of the air in the preceding theoretical equations and in the following equations for a Prandtl number of one are referred to the psuedo-surface temperature T_s'. This change in the nomenclature from reference 4 is necessary for the comparison of theory and experiment on the basis of equal values of surface-temperature parameter but for different values of Prandtl number.

For the more specific case of a cone, the surface-pressure coefficient is constant for a given Mach number, and equation (A1) becomes,

$$\delta^2 = \left[\frac{2\left(\frac{l}{\sigma^*}\right)\mu_s'}{\left(\frac{r}{l}\right) BV\rho_V}\right] \times \int_0^{s_x/l} \left(\frac{r}{l}\right)^2 d\left(\frac{s}{l}\right) \tag{A2}$$

Because the radius of a cone is a linear function of its length, the integral of equation (A2) reduces to a constant (1/3), times the length ratio $\frac{s}{l}$, or, at a given point on the surface

$$\delta^2 = \frac{1}{3}\frac{s}{l}\left[\frac{2\left(\frac{l}{\sigma^*}\right)\mu_s'}{BV\rho_V}\right] \tag{A3}$$

The Reynolds number for the flow just outside the boundary layer using the viscosity based on surface temperature is

$$Re = \frac{\rho_V V s}{\mu_s'} \tag{A4}$$

Also, since in the experimental investigation the value of air-density ratio σ^* will be one, it can be eliminated from equation (A3). With these simplifications, the laminar boundary-layer thickness relation for any cone becomes

$$\delta^2 = \frac{2}{3}\frac{s^2}{BRe} \tag{A5}$$

or

$$\delta = \frac{0.816\ s}{\sqrt{BRe}} \tag{A6}$$

The expression for surface shear per unit area for the linear velocity profile of reference 4 is

$$\tau_s = \mu_s' \frac{V}{\delta} \tag{A7}$$

Reynolds analogy between skin friction and heat transfer for

[redacted]

compressible flow gives the relation

$$\frac{\tau_s}{V} = \frac{q}{c_p(T_s - T_R)} \tag{A8}$$

or

$$q = \frac{\tau_s c_p (T_s - T_R)}{V} \tag{A9}$$

Since $Pr = \frac{c_p \mu}{k} = 1.0$, by assumption, then $T_R = T_o$ and

$$q = \frac{\tau_s k_s'(T_s' - T_o)}{\mu_s' V} \tag{A10}$$

Combining equation (A10) with equation (7) gives the relation

$$q = \frac{k_s'}{\delta}(T_s' - T_o) \tag{A11}$$

and since

$$q = h\,(T_s' - T_o) \tag{A12}$$

then

$$\frac{h\delta}{k_s'} = 1.0 = Nu_\delta \tag{A13}$$

With the laminar boundary-layer-thickness relation and the boundary-layer Nusselt number relation known, the two can be combined to give values of local heat-transfer coefficients directly,

$$h = \frac{k_s'\sqrt{B\ Re}}{0.816s} \tag{A14}$$

or in terms of local Nusselt number

$$Nu = \frac{hs}{k_s'} = 1.225\sqrt{B\ Re} \tag{A15}$$

APPENDIX B

AVERAGE HEAT-TRANSFER COEFFICIENTS

The local rate of heat transfer in the laminar boundary-layer region of a cone can be expressed in equation (A14) as

$$h = \frac{c_1}{\sqrt{s}} \tag{B1}$$

and the incremental area over which the local heat-transfer coefficient is applied can be shown to be

$$dA = c_2 s \, ds \tag{B2}$$

The average value of the heat-transfer coefficient is then given by the relation

$$\bar{h} = \frac{\int_0^s h \, dA}{\int_0^s dA} = \frac{c_1(c_2)\int_0^s \sqrt{s} \, ds}{c_2 \int_0^s s \, ds} \tag{B3}$$

or

$$\bar{h} = c_1 \frac{\frac{2}{3} s^{3/2}}{\frac{1}{2} s^2} = \frac{\frac{4}{3} c_1}{\sqrt{s}} \tag{B4}$$

but, since

$$h = c_1/\sqrt{s}$$

then

$$\bar{h} = \frac{4}{3} h \tag{B5}$$

This relation has also been obtained, in a slightly different form, by Hantzsche and Wendt in reference 5.

[redacted]

[redacted]

APPENDIX C

COMPARISON WITH INCOMPRESSIBLE-FLOW THEORY

For a flat plate, the laminar boundary-layer-thickness relation of reference 7 reduces to the form

$$\delta^2 = \frac{5.3s^2}{Re} \tag{C1}$$

for the boundary-layer thickness measured at the point in the velocity profile where the dynamic pressure is one-half of free-stream dynamic pressure. Also, in reference 7, it is shown that for the Blasius velocity profile the boundary-layer Nusselt number is given by the relation

$$Nu_\delta = \frac{h\delta}{k} = 0.765 \tag{C2}$$

The following relation is obtained from the method of reference 4 for the boundary-layer thickness measured at the same point in the velocity profile:

$$\delta^2 = \frac{2s^2}{B\ Re} \tag{C3}$$

and

$$Nu_\delta = \frac{h\delta}{k_s'} = 1.0 \tag{C4}$$

Combining and rearranging equations (C1) and (C2) gives the relation

$$h = 0.322k\sqrt{\frac{Re}{s^2}} \tag{C5}$$

Similarly, equations (C3) and (C4) yield the relation

$$h = \sqrt{\frac{B}{2}}\,k\sqrt{\frac{Re}{s^2}} \tag{C6}$$

[redacted]

For a Mach number of zero, and zero heat transfer $(\beta = 1.0)$, $k = k_s'$ and

$$h = 0.286k\sqrt{\frac{Re}{s^2}} \tag{C7}$$

A comparison of the constants of equations (C5) and (C7) is indicative of the effect of the linear-velocity-profile assumption.

APPENDIX D

METHOD OF CALCULATION AND DESIGN CHARTS

The value of the surface-temperature parameter can be calculated from the known boundary-layer conditions by the relation (for Prandtl number = 0.73).

$$\beta_{0.73} = \frac{T_s - T_v}{T_R - T_v} \tag{D1}$$

where

$$T_R = T_v\left(1 + \sqrt{Pr}\,\frac{\gamma - 1}{2}\,M_v^2\right) \tag{D2}$$

With a Prandtl number of unity as is assumed in the theory

$$\beta_{1.0} = \frac{T_s' - T_v}{T_o - T_v} \tag{D3}$$

In order to have similar temperature profiles in the actual and theoretical cases, the surface-temperature parameters must be equal.

$$\beta_{1.0} = \beta_{0.73} \tag{D4}$$

Therefore, the pseudo-surface temperature is given by the relation

$$T_s' = \beta(T_o - T_v) + T_v \tag{D5}$$

or

$$T_s' = \frac{T_s - T_v}{\sqrt{Pr}} + T_v \tag{D6}$$

because

$$\sqrt{Pr} = \frac{T_R - T_v}{T_o - T_v} \tag{D7}$$

With the values of surface-temperature parameter and pseudo-surface temperature known, the values of the parameter B, the viscosity, and the thermal conductivity of air at the surface based on the pseudo-surface temperature can be determined. This, in turn, allows the Reynolds number corresponding to the desired position on the cone to be calculated

$$Re = \frac{\rho_v V s}{\mu_s'} \tag{D8}$$

With the values of B and Reynolds number known, the local Nusselt number can easily be determined by equation (A15). The local heat-transfer coefficient can be determined from the local Nusselt number by the relation

$$h = Nu \frac{k_s'}{s} \tag{D9}$$

The theoretical results presented were calculated from the foregoing relations. The conditions of the air stream just outside the boundary layer were obtained by the use of reference 9, rather than by the linearized theory of reference 10 as indicated in reference 4. With this change, the limit of applicability of the method is not the extreme body fineness ratio dictated by linearized theory, but rather the Mach number for nose shock-wave detachment. The change in limiting fineness ratio requires the length s in the foregoing equations to be taken as the slant length because the assumption in reference 4 that the surface and axial lengths are equal is not valid for blunt bodies.

The following outline gives a step-by-step procedure for calculating the rate of heat transmission to a cone moving at constant supersonic velocity. Use is made of the charts of this

report (fig. 18) which were developed from the theory set forth in reference 4. Table II of reference 9 is very useful in many of the calculations, and its application is indicated in the appropriate steps. However, the symbols used in reference 9 differ from those used in reference 4 and the present report. A table of equivalent symbols follows:

Present report and reference 4	Reference 9
T/T_o	T/T_a
T_v/T_o	T/T_a at $M = M_v$
ρ_v/ρ_o	ρ/ρ_a at $M = M_v$
a_v/a_o	a/a_a at $M = M_v$

To begin the calculations the following information must be known:

M flight Mach number

T ambient static air temperature, $^{\circ}F$ absolute

T_s surface temperature to be maintained on the cone, $^{\circ}F$ absolute

θ_c half-angle of the cone, degrees

p ambient-air pressure, pounds per square foot

The calculations then proceed with the determination of the following parameters:

1. Total temperature T_o

$$\frac{T_o}{T} = \left(1 + \frac{\gamma-1}{2} M^2\right)$$

or, enter table II of reference 9 with M and find T/T_o directly. (See the preceding table for equivalent symbols.)

[redacted]

2. Mach number just outside the boundary layer of the cone M_v. Enter figure 18(a) with M and θ_c and determine M_v/M. (This figure is taken from reference 11.)

3. Temperature of the air stream just outside the cone boundary layer T_v,

$$\frac{T_v}{T_o} = \left(1 + \frac{\gamma-1}{2} M_v^2\right)^{-1}$$

or, enter table II of reference 9 with $M = M_v$ and find T_v/T_o directly.

4. Recovery surface temperature T_R. Enter figure 18(b) with M_v and determine T_R/T_o.

5. Surface-temperature parameter β,

$$\beta = \frac{T_s - T_v}{T_R - T_v}$$

6. Pseudo-surface temperature T_s',

$$T_s' = \beta(T_o - T_v) + T_v$$

7. Total pressure behind bow shock wave H_1. The total pressure ahead of the bow shock wave H_o is given by

$$\frac{H_o}{p} = \left(1 + \frac{\gamma-1}{2} M^2\right)^{\frac{\gamma}{\gamma-1}}$$

or, enter table II of reference 9 with M and find p/H directly. Then

$$\frac{H_1}{H_o} = \left[\frac{(\gamma+1)M^2 \sin^2\theta}{(\gamma-1)M^2 \sin^2\theta + 2}\right]^{\frac{\gamma}{\gamma-1}} \left[\frac{2\gamma M^2 \sin^2\theta - (\gamma-1)}{\gamma+1}\right]^{-\frac{1}{\gamma-1}}$$

where θ is the bow shock-wave angle and can be determined from figure 7 of reference 9.

8. Density at total pressure behind the bow shock wave ρ_o,

$$\rho_{o_1} = \frac{H_1}{RT_o}$$

9. Density just outside the cone boundary layer ρ_V

$$\frac{\rho_V}{\rho_{o_1}} = \left(1 + \frac{\gamma-1}{2} M_V^2\right)^{\frac{1}{\gamma-1}}$$

or, enter table II of reference 9 with $M = M_V$ and find ρ_V/ρ_{o_1} directly.

10. Velocity of sound at total temperature conditions a_o

$$a_o^2 = \gamma R T_o$$

11. Velocity of air stream just outside the boundary layer of the cone V,

$$\left(\frac{V}{a_o}\right)^2 = \frac{M_V^2}{1 + \frac{\gamma-1}{2} M_V^2}$$

or, enter table II of reference 9 with $M = M_V$ and find a_V/a_o then $V = M_V \times a_V$.

12. Absolute viscosity at the surface of the cone μ_s'. Enter figure 18(c) with $(T_s'-460)$ and determine μ_s'.

13. Reynolds number per foot of slant length Re/s.

$$\frac{Re}{s} = \frac{\rho_V V}{\mu_s'}$$

14. Reynolds number for various positions on the surface of the cone Re.

(a) Choose stations along the surface of the cone at which it is desired to determine local heat-transfer rates.

(b) Measure the distances s along the surface of the cone from the apex to the stations in feet.

(c) Then, the Reynolds number is equal to $\left(\frac{Re}{s}\right) \times s$ for each station.

15. Local Nusselt number for each station Nu.

(a) Enter figure 18(d) with M_V and β and determine $Nu/\sqrt{Re}$.

(b) The local Nusselt number for each station is then found by multiplying this value by the square root of the Reynolds numbers for the respective stations.

16. Local heat-transfer coefficient h.

(a) Enter figure 18(e) with $T_s'-460$ and find the thermal conductivity of air at the surface of the cone k_s'.

(b) Then, h is equal to $\frac{Nu\ k_s'}{s}$ for each station.

17. Local rate of heat transfer q.

$$q = h(T_s - T_R)$$

18. Average heat-transfer coefficient $\bar{h}$. The average coefficient for that portion of the cone from the apex to any point along its surface for laminar flow is given by $\bar{h} = (4/3)h$.

REFERENCES

1. Owen, P. R.: Note on the Apparatus and Work of the W.V.A. Supersonic Institute at Kochel, S. Germany, Part IV – Important Results. RAE Tech. Note Aero. 1742. Jan. 1946.

2. Lees, Lester: The Stability of the Laminar Boundary Layer in a Compressible Fluid. NACA TN No. 1360, 1947.

3. Liepmann, Hans W., and Fila, Gertrude H.: Investigations of Effects of Surface Temperature and Single Roughness Elements on Boundary-Layer Transition. NACA TN No. 1196, 1947.

4. Scherrer, Richard: The Effects of Aerodynamic Heating and Heat Transfer on the Surface Temperature of a Body of Revolution in Steady Supersonic Flight. NACA TN No. 1300, 1947.

5. Hantzsche, W., and Wendt, H.: The Laminar Boundary Layer of the Flat Plate with and Without Heat Transfer Considering Compressibility. Jahrbuck der Deutschen Luftfahrtforschung, 1942, Part I, pp. 40–50.

6. von Kármán, Th., and Tsien, H. S.: Boundary Layers in Compressible Fluids. Jour. Aero. Sci., vol. 5, no. 6, Apr. 1938, pp. 227–232.

7. Allen, H. Julian, and Look, Bonne C.: A Method for Calculating Heat Transfer in the Laminar Flow Region of Bodies. NACA Rep. No. 764, 1943.

8. Michels, Walter C.: Advanced Electrical Measurements. Second Edition. D. Van Nostrand Company (New York), 1943, p. 11.

9. Staff of Ames 1- by 3-foot Supersonic Wind-Tunnel Section: Notes and Tables for Use in the Analysis of Supersonic Flow. NACA TN No. 1428, 1947.

10. von Kármán, Th., and Moore, N. B.: Resistance of Slender Bodies Moving with Supersonic Velocities with Special Reference to Projectiles. A.S.M.E. (Applied Mech.) Dec. 15, 1932, pp. 303–310.

11. Moeckel, W.E., and Connors, J. F.: Charts for the Determination of Supersonic Airflow Against Inclined Planes and Axially Symmetric Cones. NACA TN No. 1373, 1947.

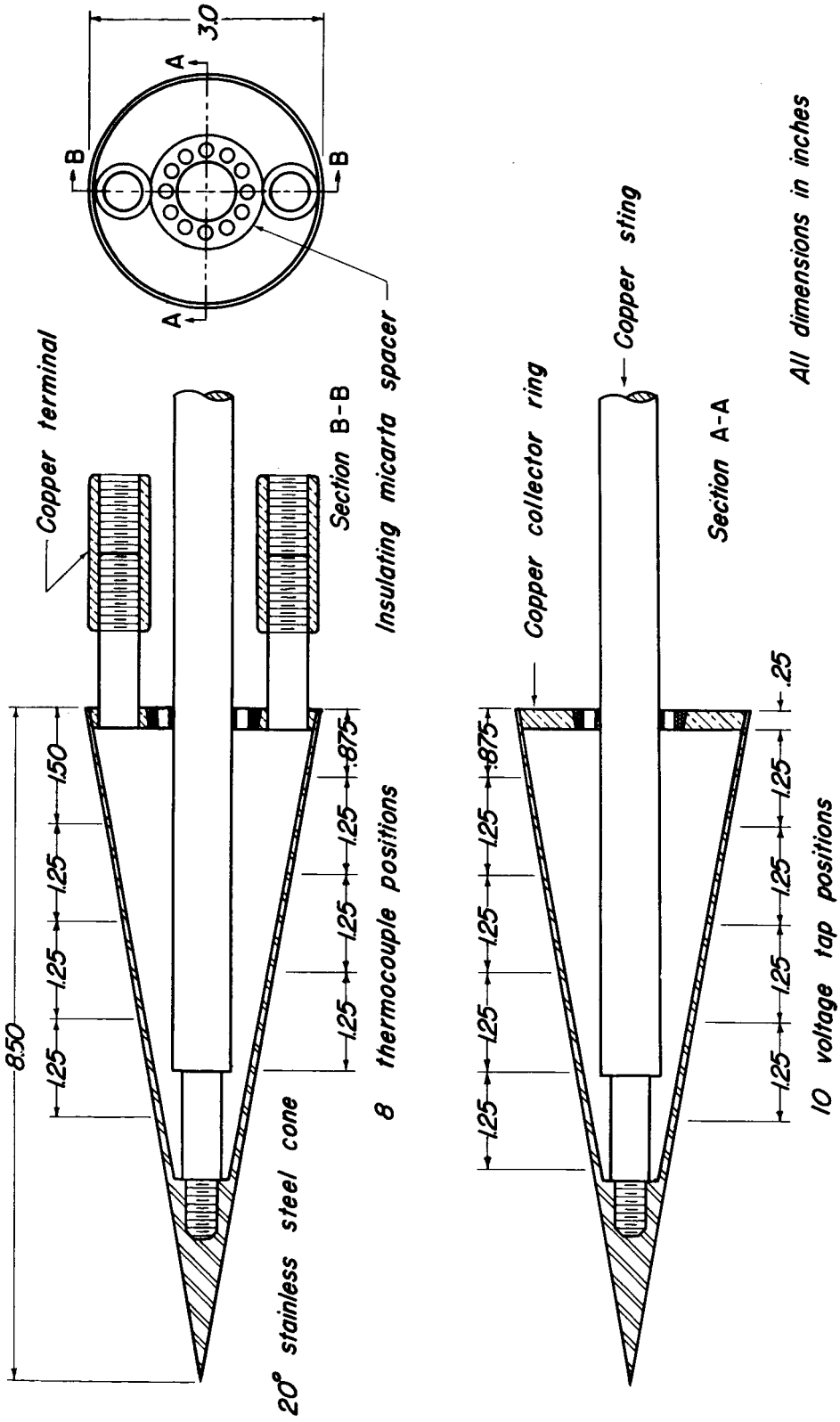

Figure 1.-Design details of the 20° cone.

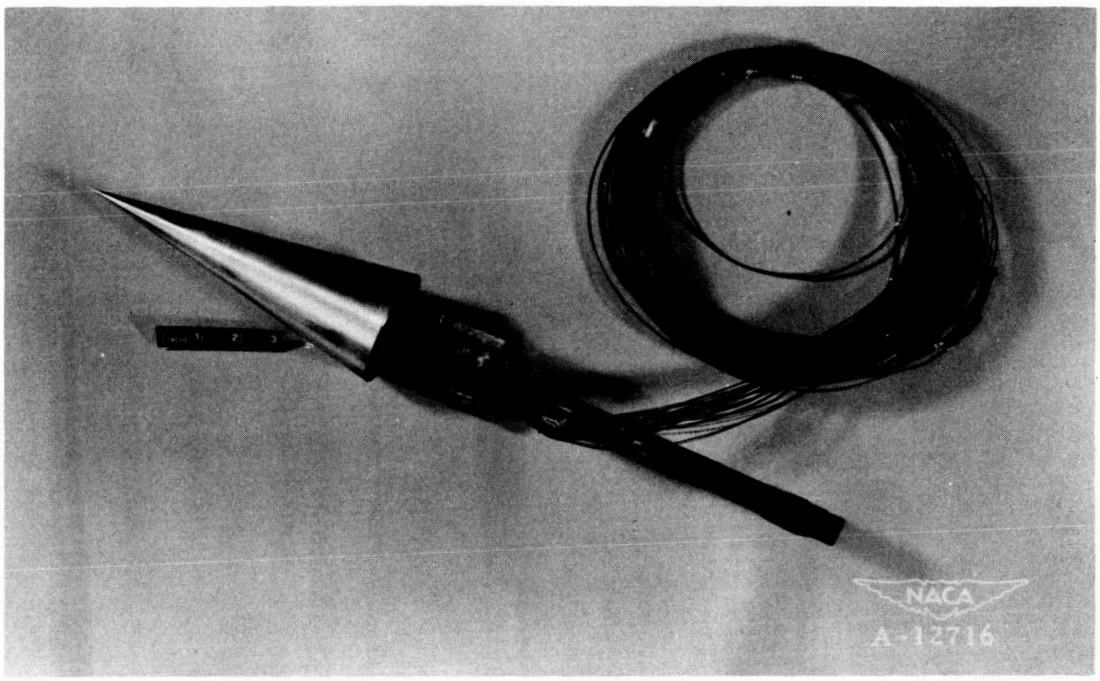

Figure 2.– Electrically heated 20° cone with power terminals, voltage-tap leads and thermocouple leads.

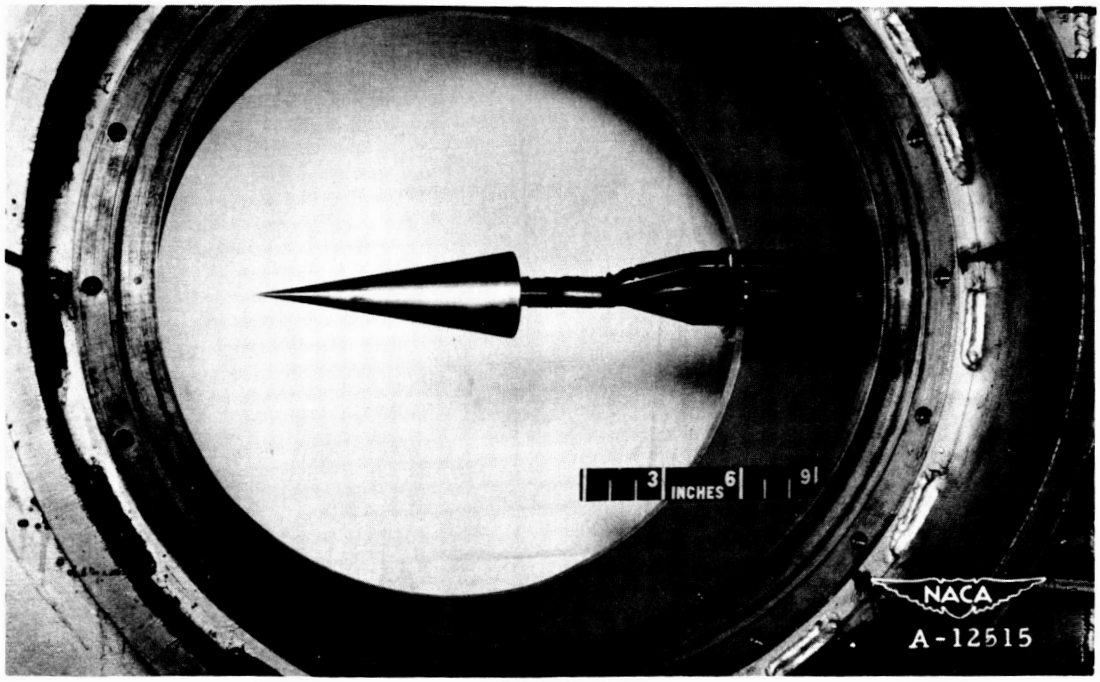

Figure 3.– Heated 20° cone installed in the test section of the Ames 1- by 3-foot supersonic wind tunnel No. 1.

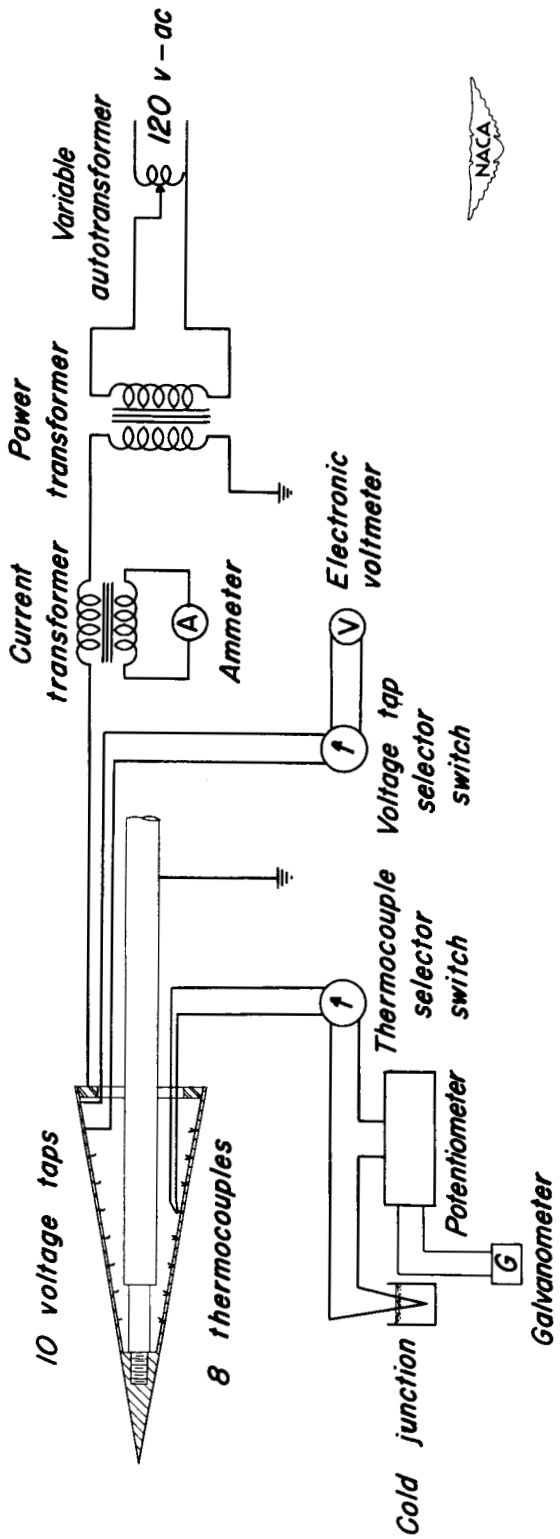

Figure 4.- Simplified wiring diagram for electrically heated cone.

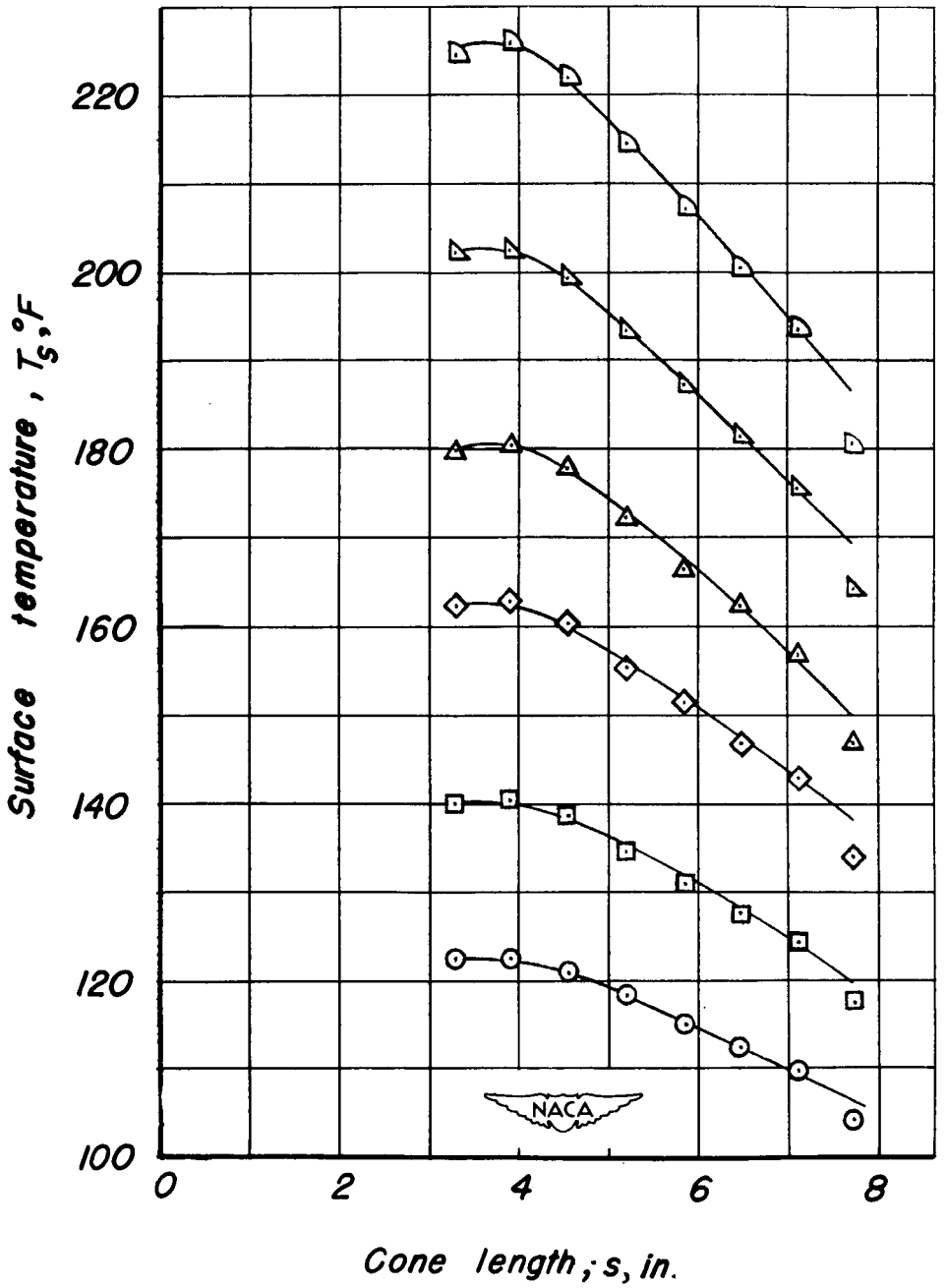

(a) H_0 = 3.1 lb/sq in. abs.

Figure 5.—Surface-temperature distributions for various nominal surface temperatures on the heated 20° cone with a laminar boundary layer.

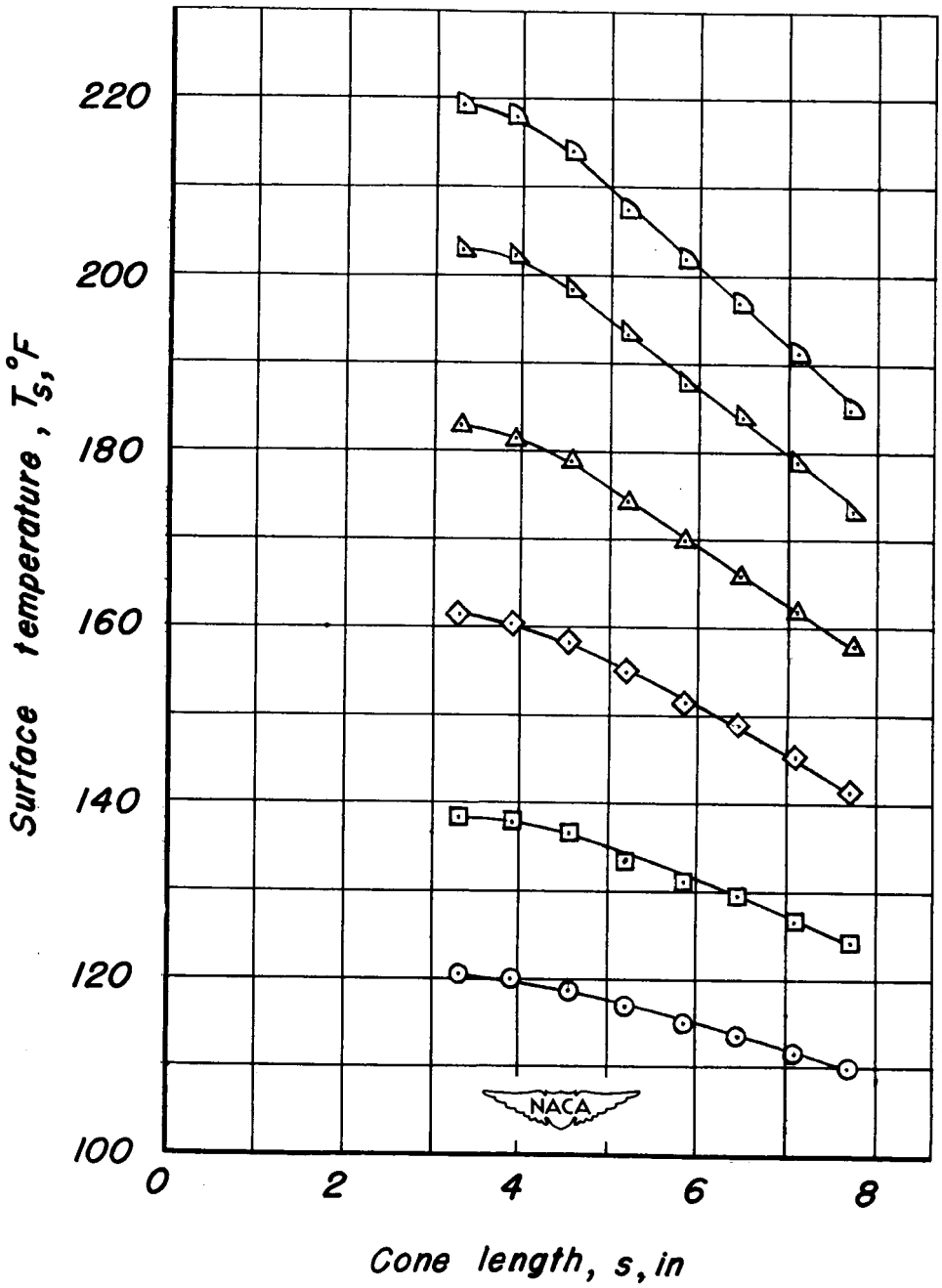

(b) H_o = 5.7 lb/sq in. abs.

Figure 5.- Continued.

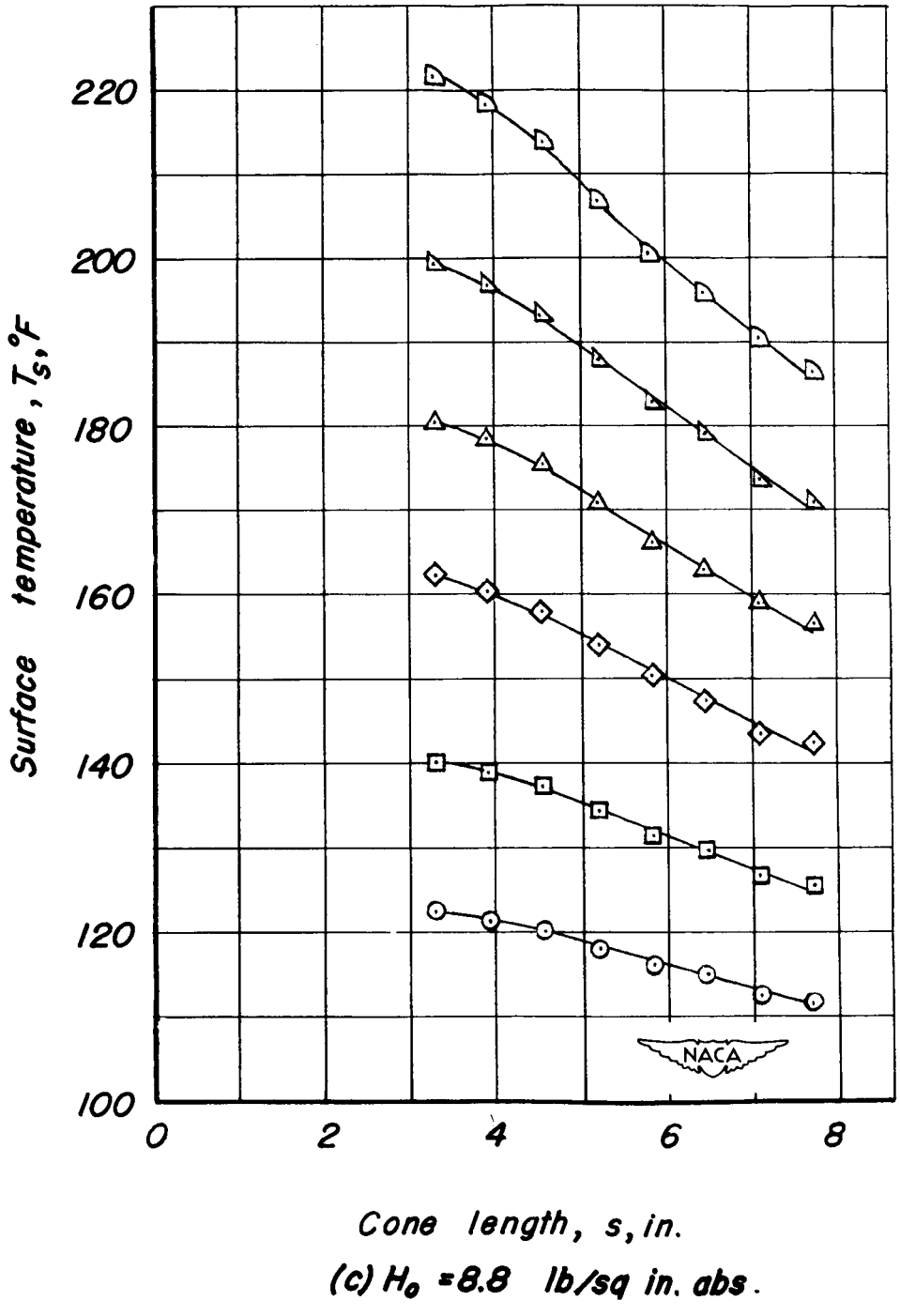

(c) H_o = 8.8 lb/sq in. abs.

Figure 5.—Continued.

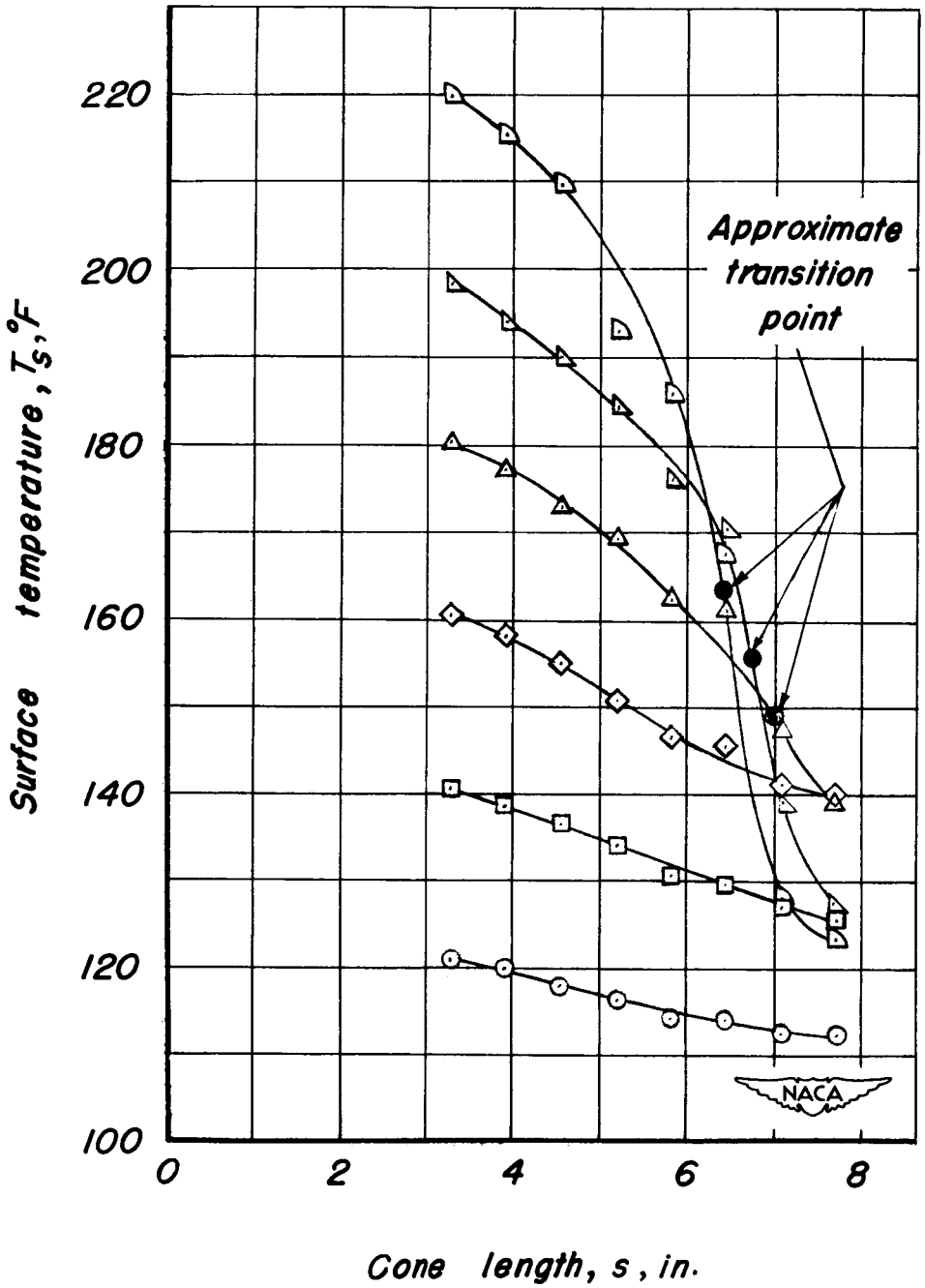

(d) H_0 = 14.8 lb/sq in. abs.

Figure 5.- Continued.

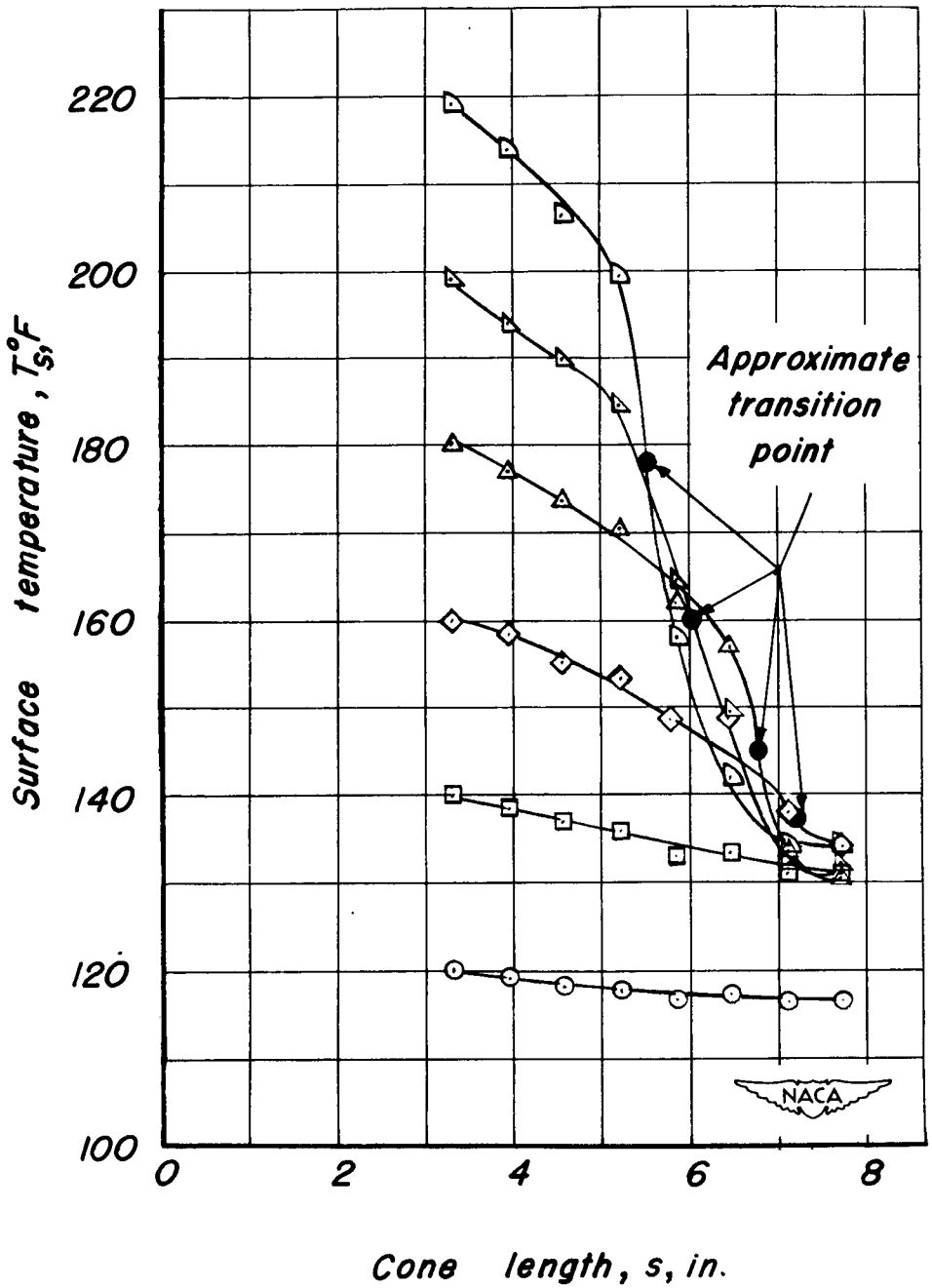

(e) H_o = 21.0 lb/sq in. abs.

Figure 5.– Concluded.

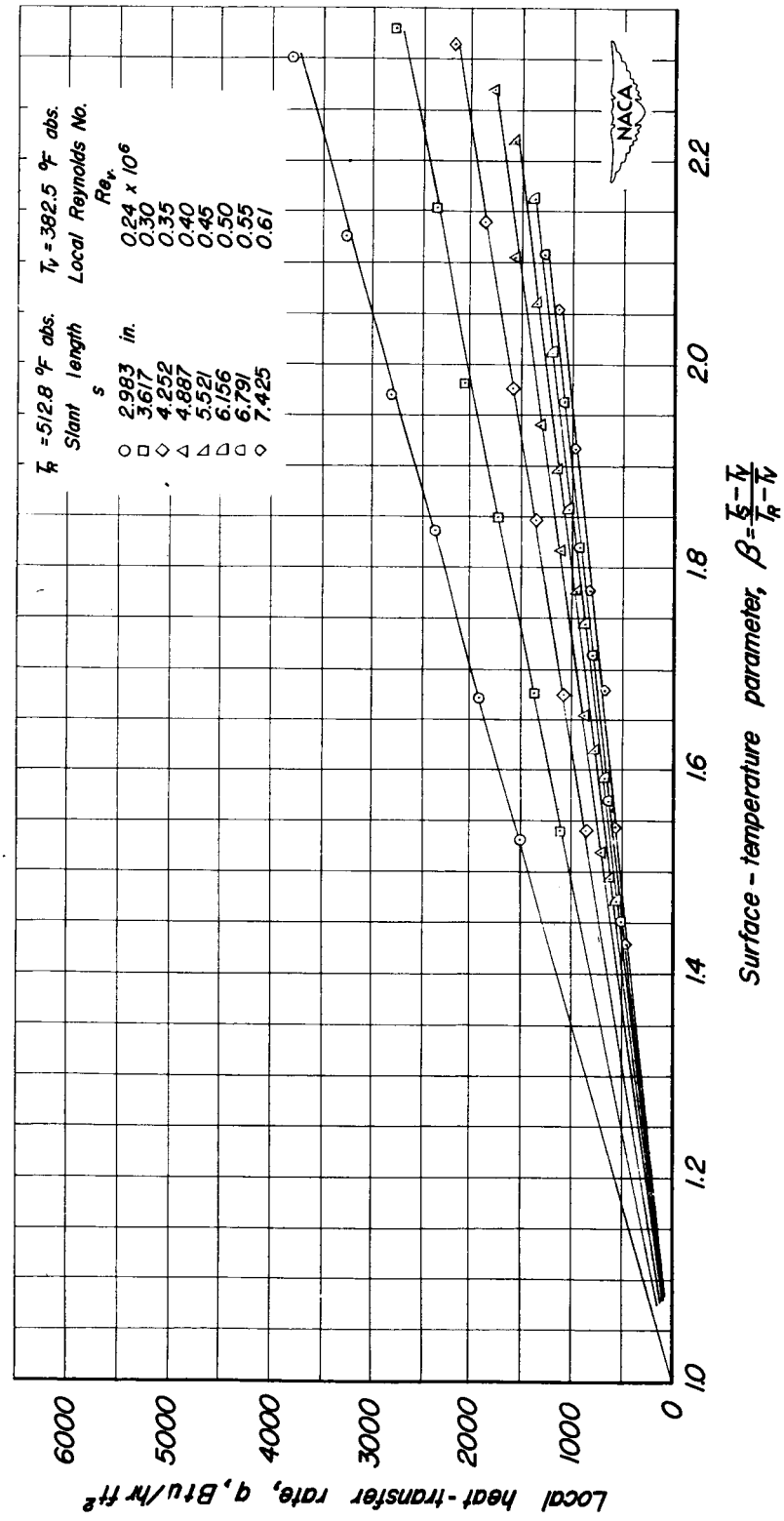

(a) H_o = 3.1 lb/sq in. abs.

Figure 6.—The variation of the local rate of heat transfer with surface-temperature parameter for successive positions along the length of the 20° cone.

[redacted]

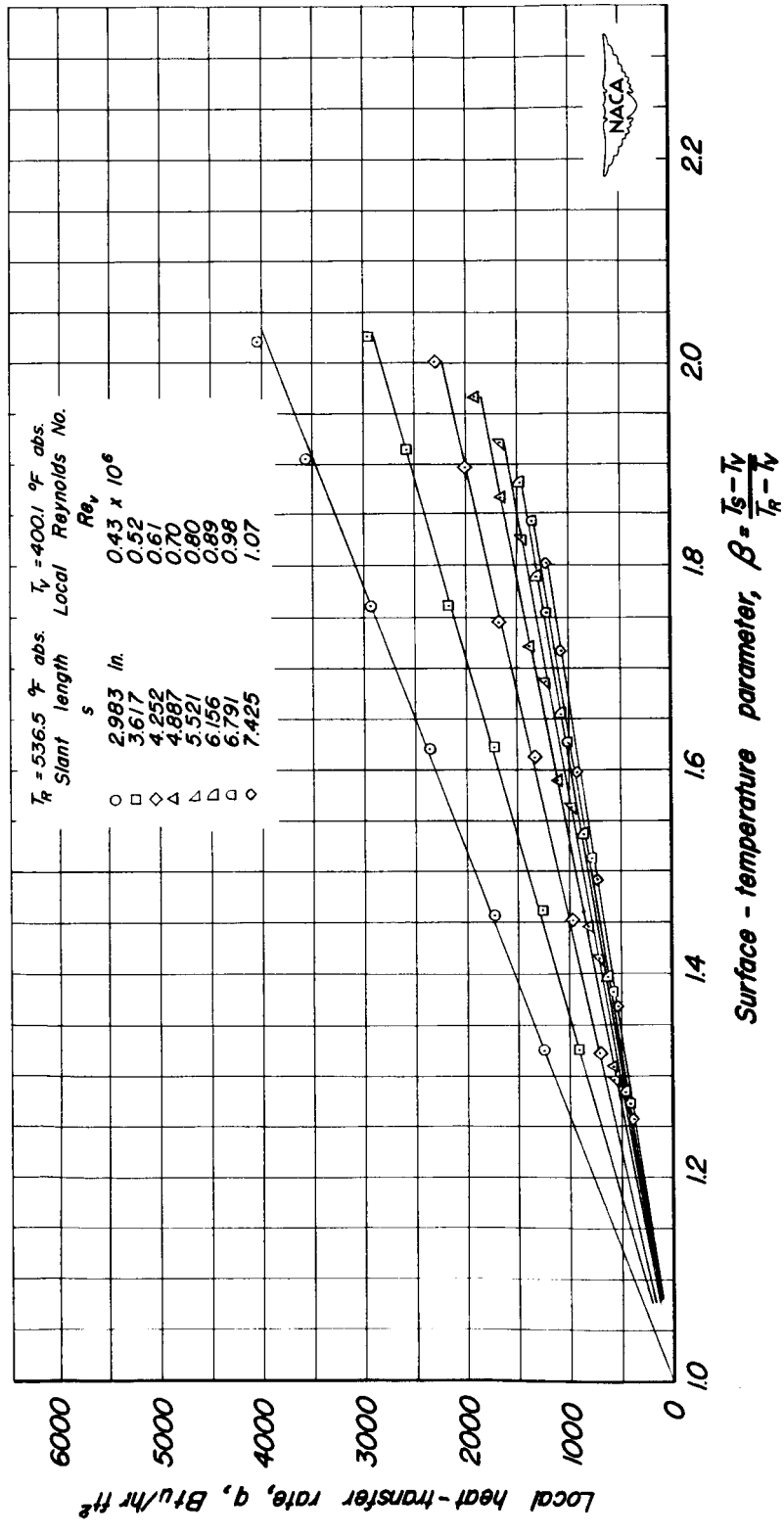

(b) H_o = 5.7 lb/sq. in. abs.

Figure 6.—Continued.

[redacted]

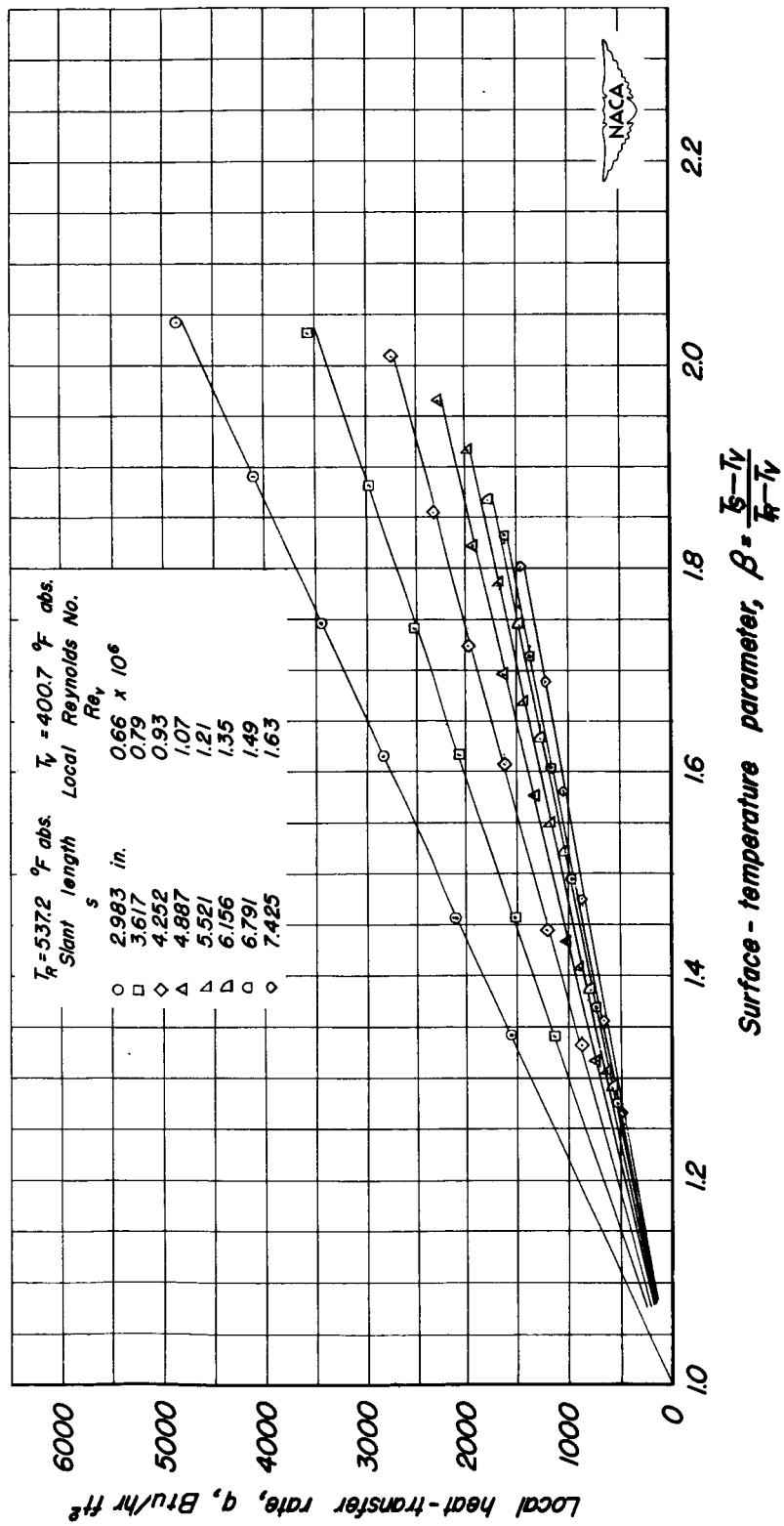

(c) H_o = 8.8 lb/sq in. abs.

Figure 6.—Continued.

[redacted]

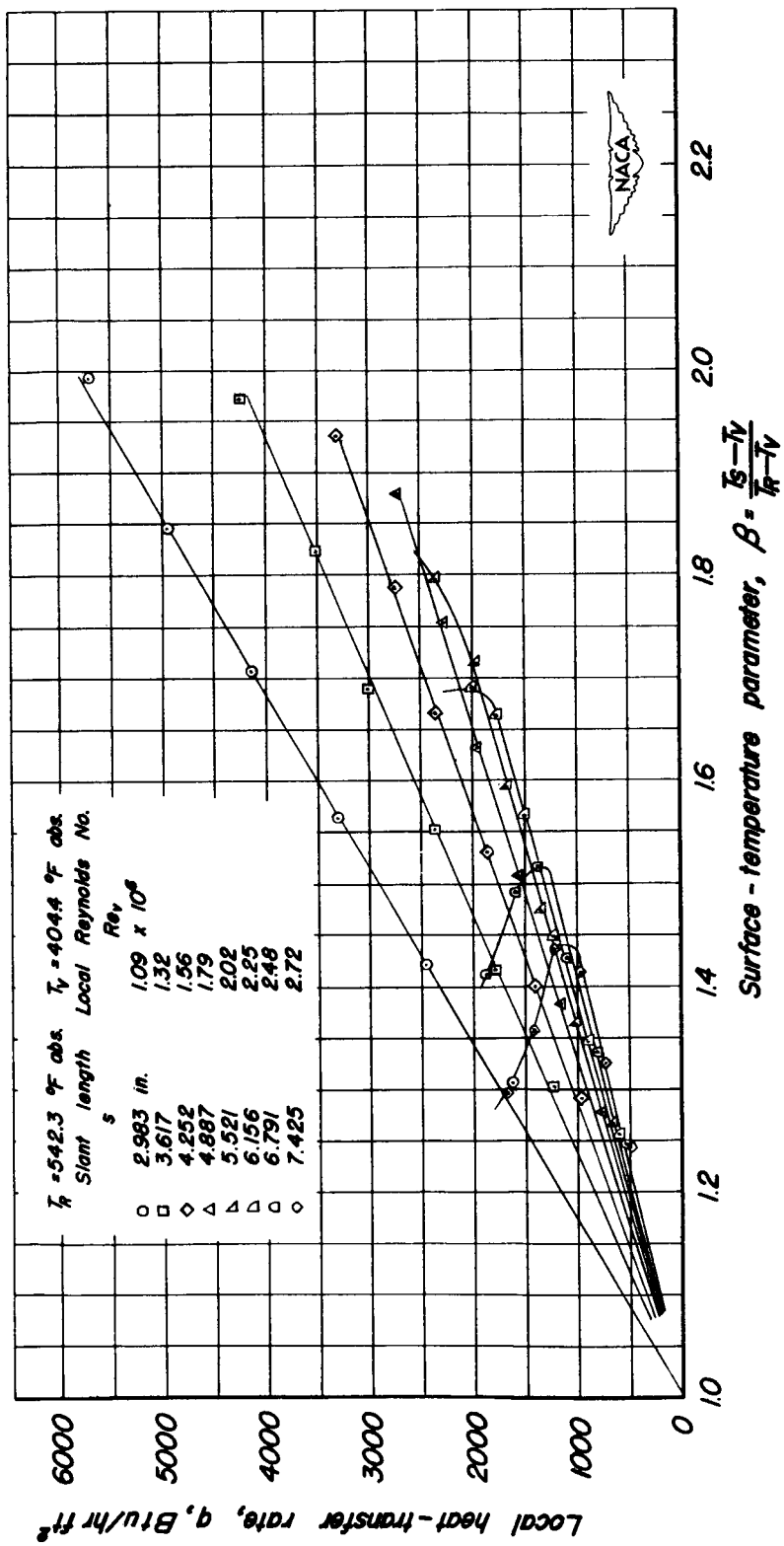

(d) H_o = 14.8 lb/sq in. abs.

Figure 6.—Continued.

[redacted]

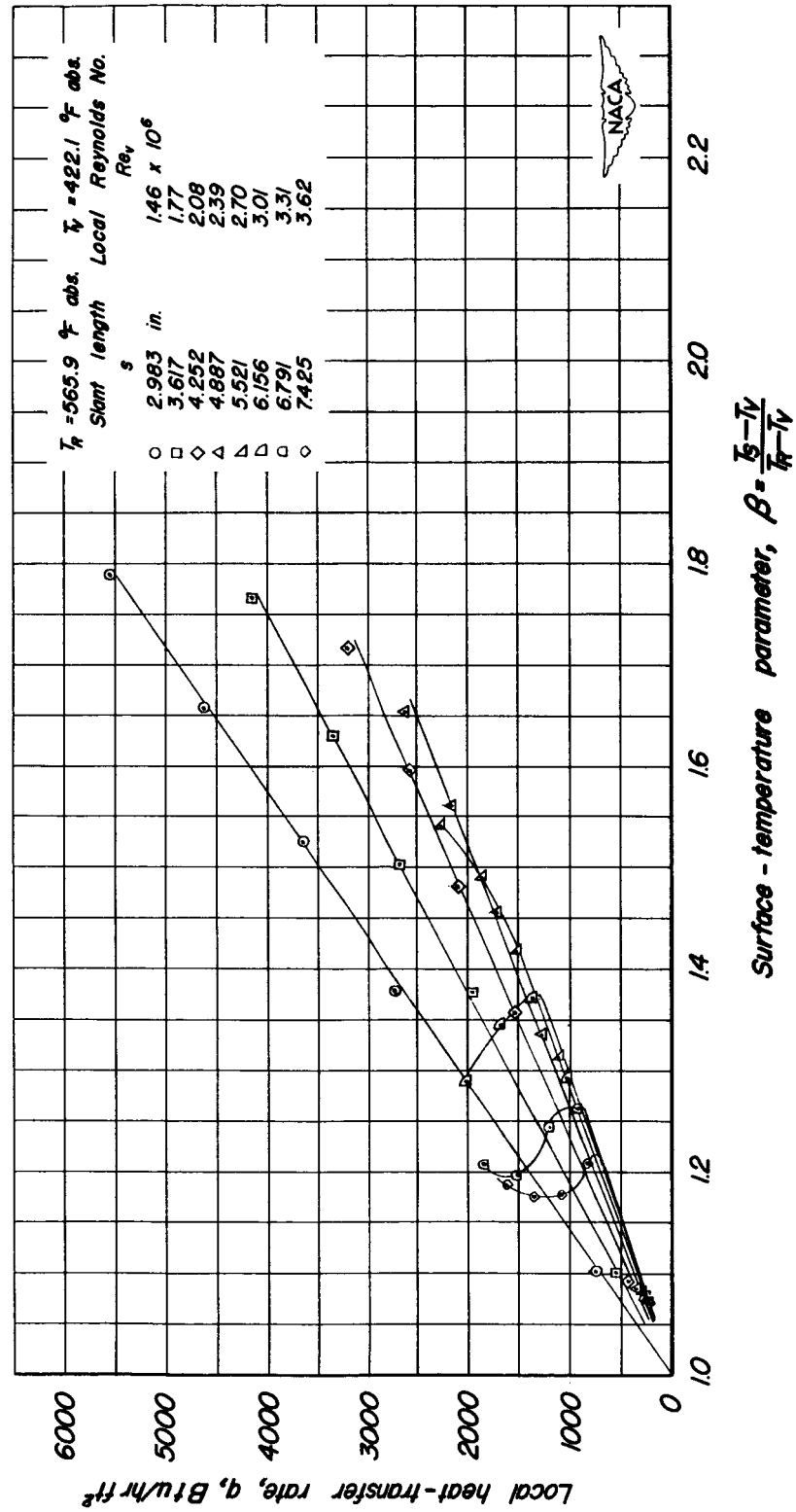

(e) H_o = 21.0 lb/sq in. abs.

Figure 6.—Concluded.

[redacted]

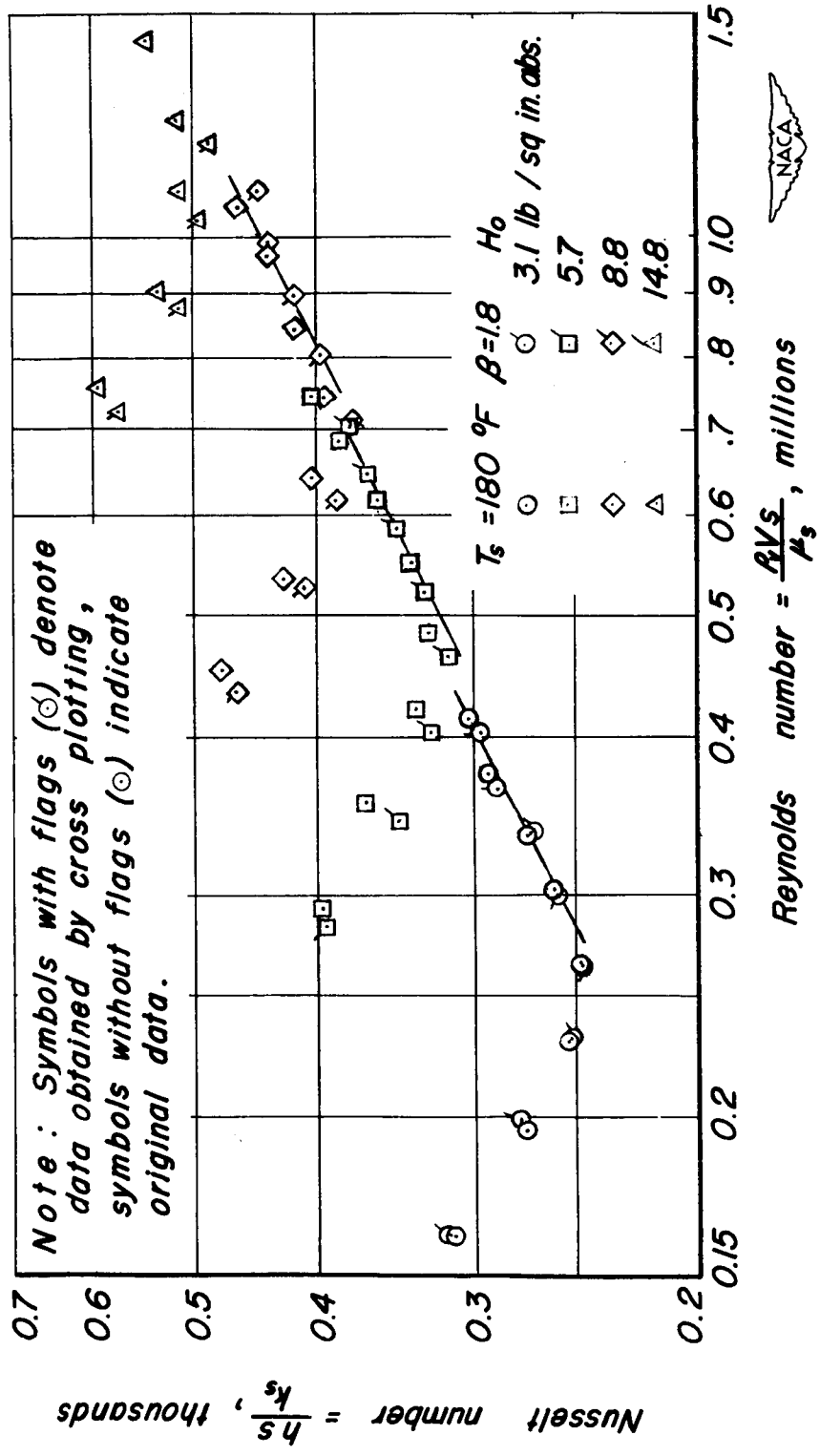

Figure 7. – A comparison of the results obtained with and without the assumption of a negligible surface-temperature gradient.

[redacted]

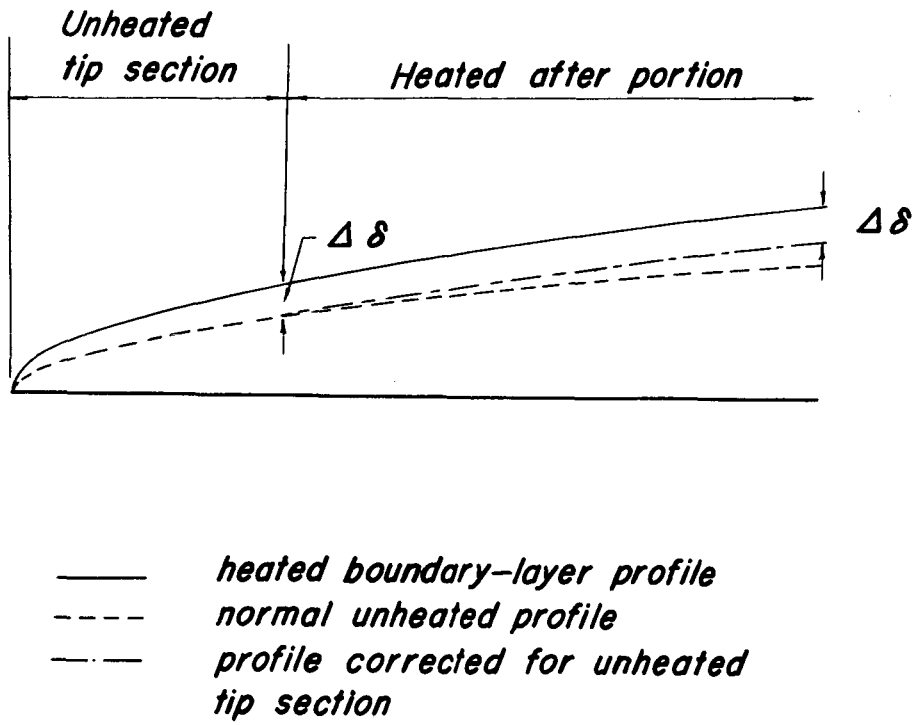

Figure 8.— Diagram of the method of correcting the laminar boundary-layer thickness for the effect of the unheated nose of the 20° cone.

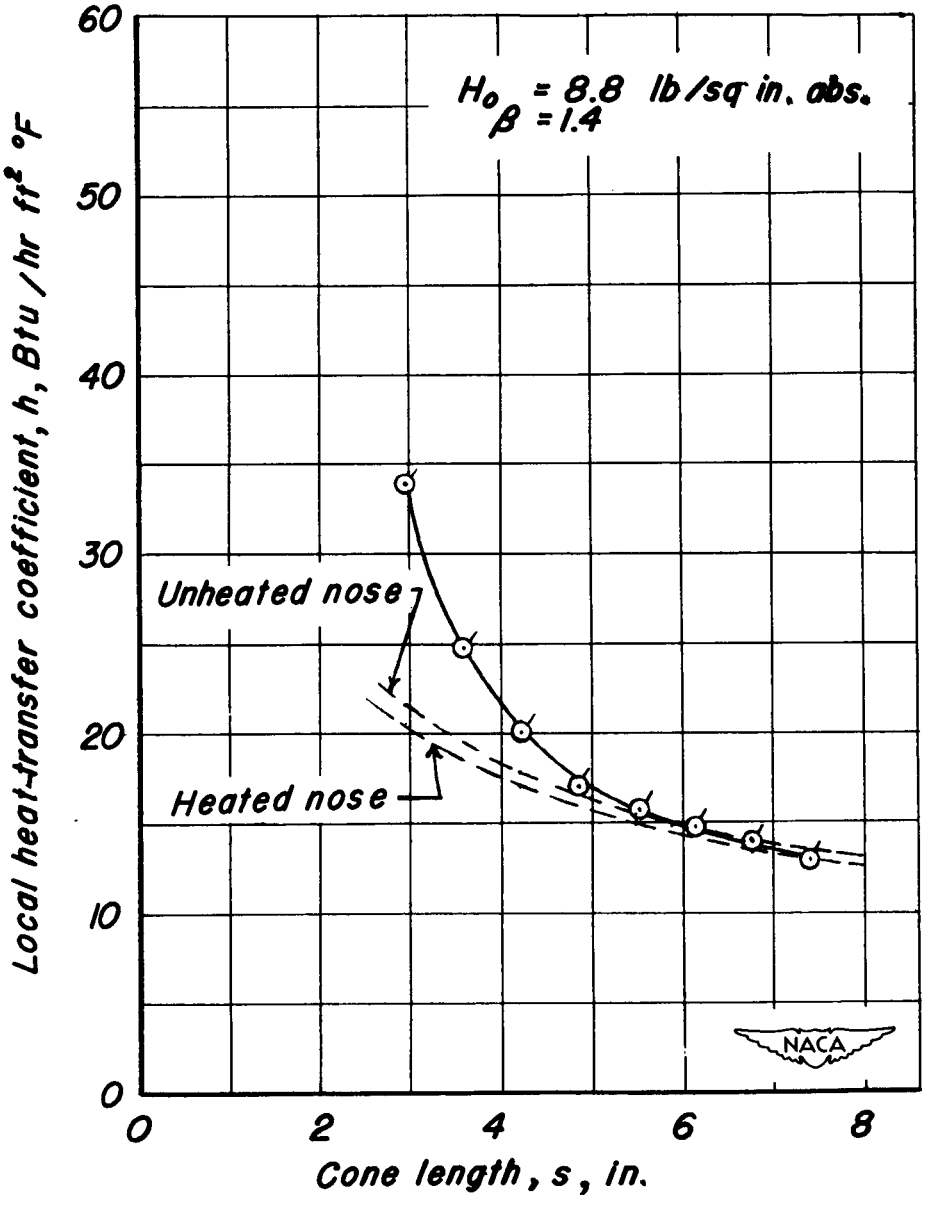

Figure 9. — A comparison of experimental laminar heat-transfer-coefficient distribution on a 20° cone and the theoretical distributions for both the heated and unheated nose conditions.

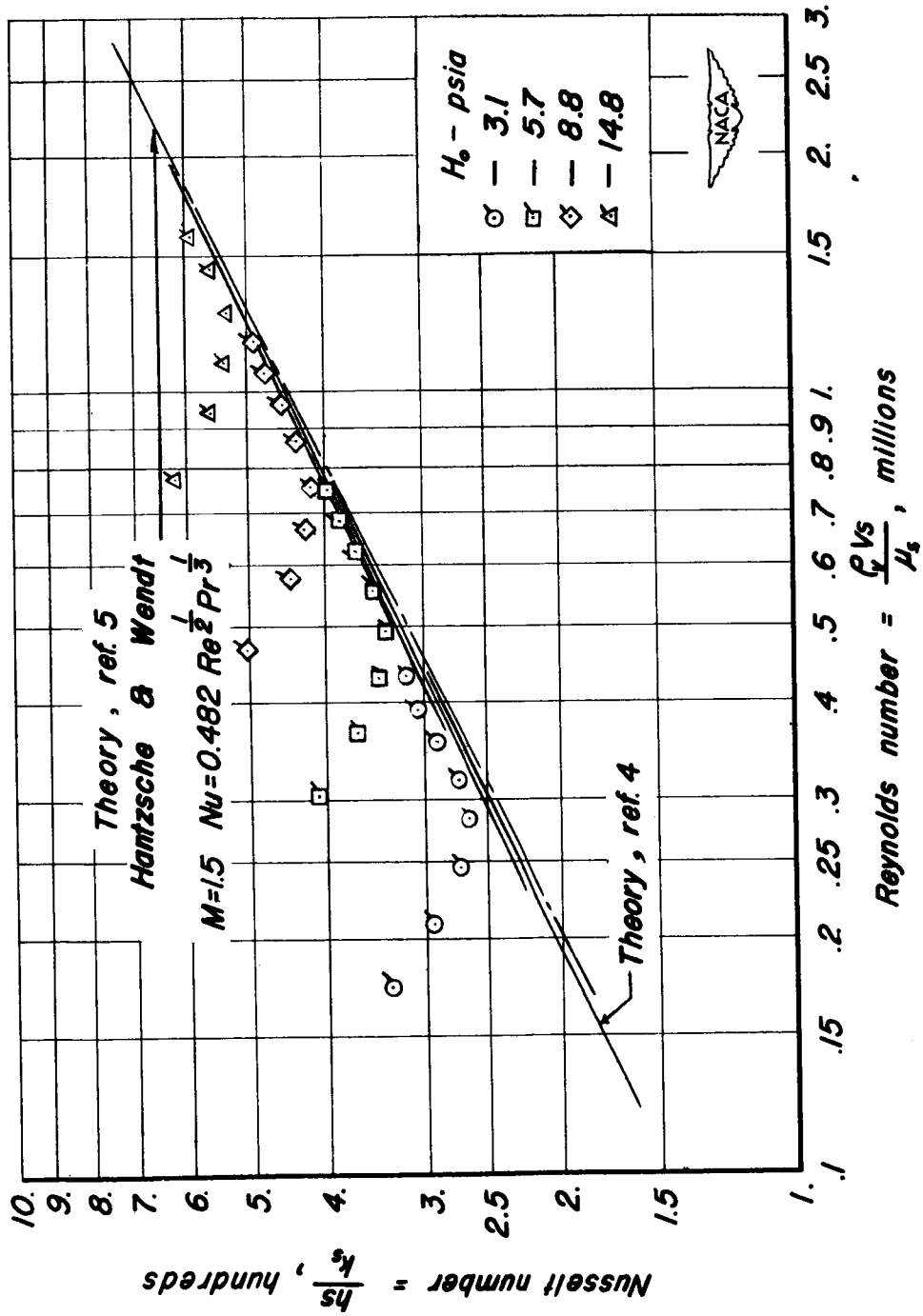

(a) $\beta = 14$.

Figure 10.— The variation of local Nusselt number with length Reynolds number for a laminar boundary layer on the heated 20° cone.

[redacted]

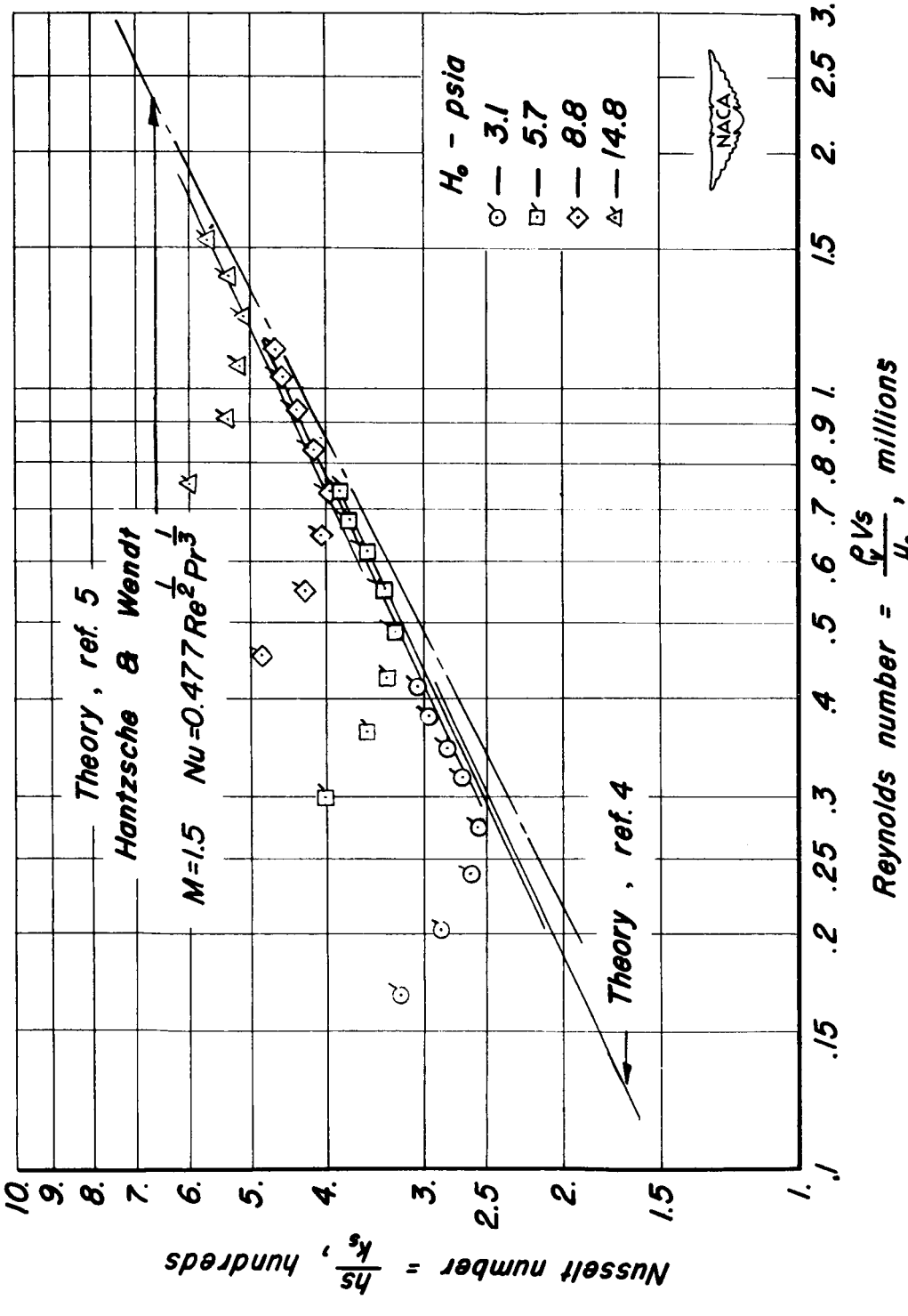

(b) $\beta = 1.6$.

Figure 10.—Continued.

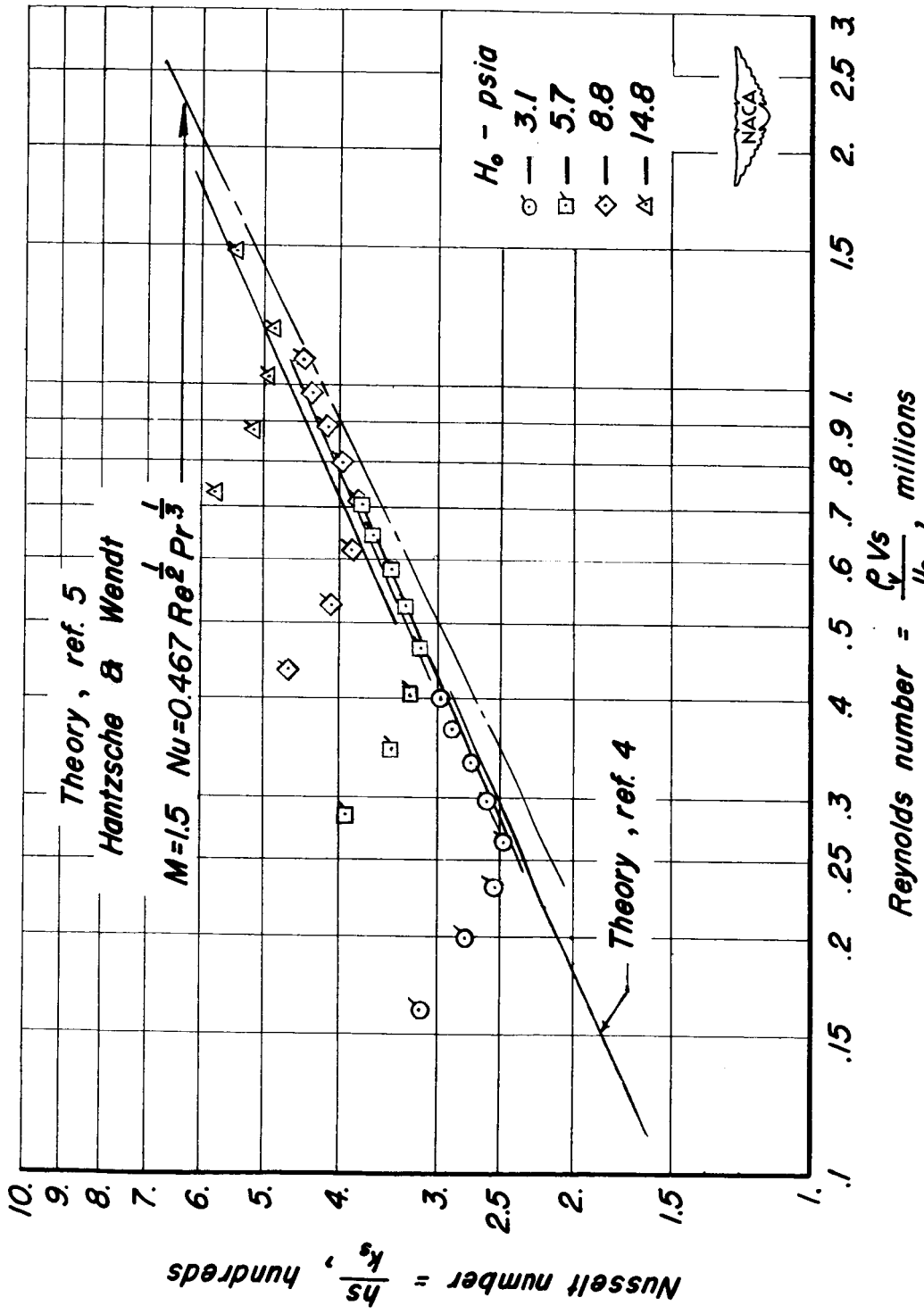

(c) $\beta = 1.8$.

Figure 10.—Continued.

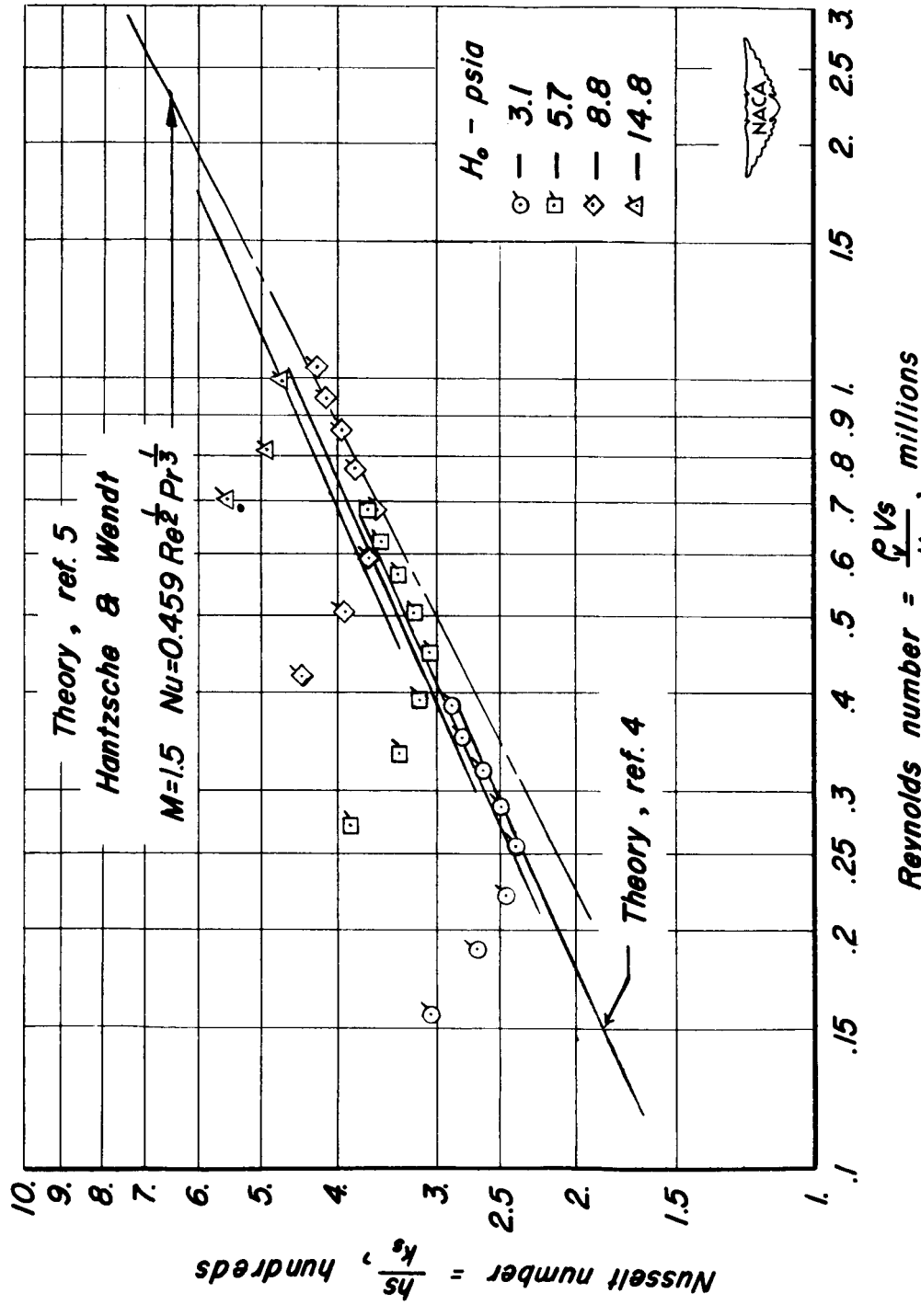

(d) $\beta = 2.0$.

Figure 10.—Concluded.

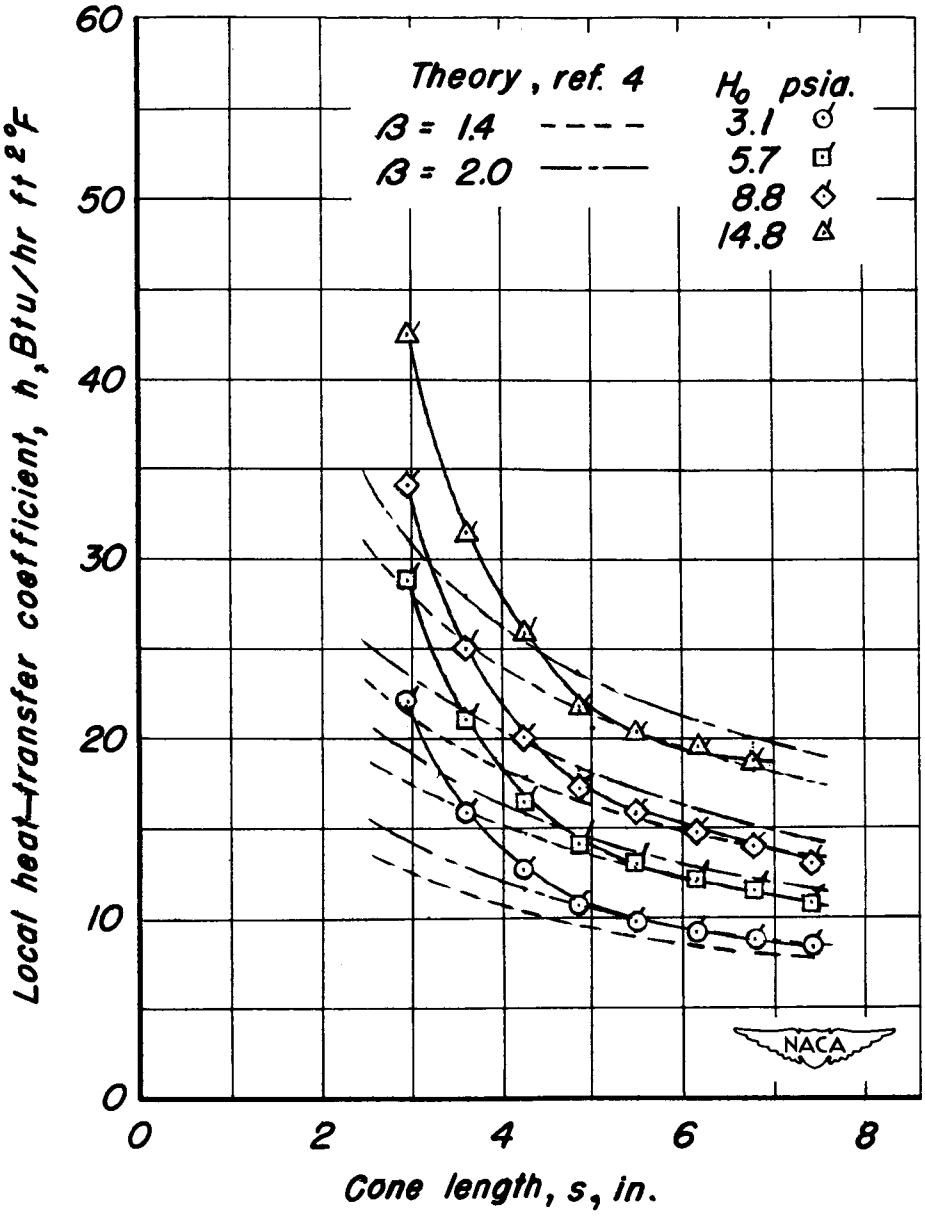

Figure 11. — A comparison of the theoretical laminar heat-transfer-coefficient distributions on a 20° cone with the experimental distributions.

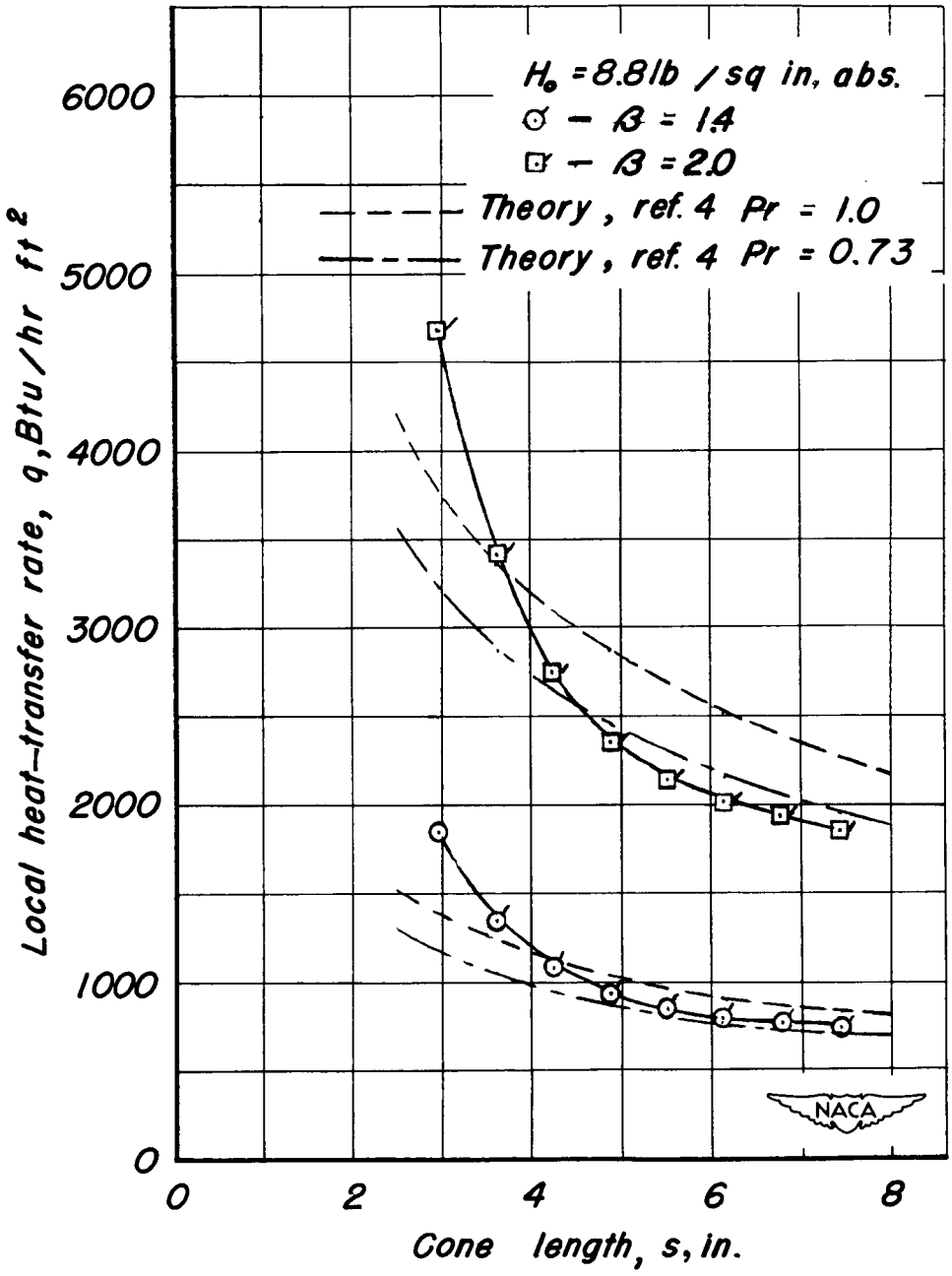

Figure 12. — Comparison of the experimental local heat-transfer-rate distribution with that calculated by the theory for laminar boundary layers.

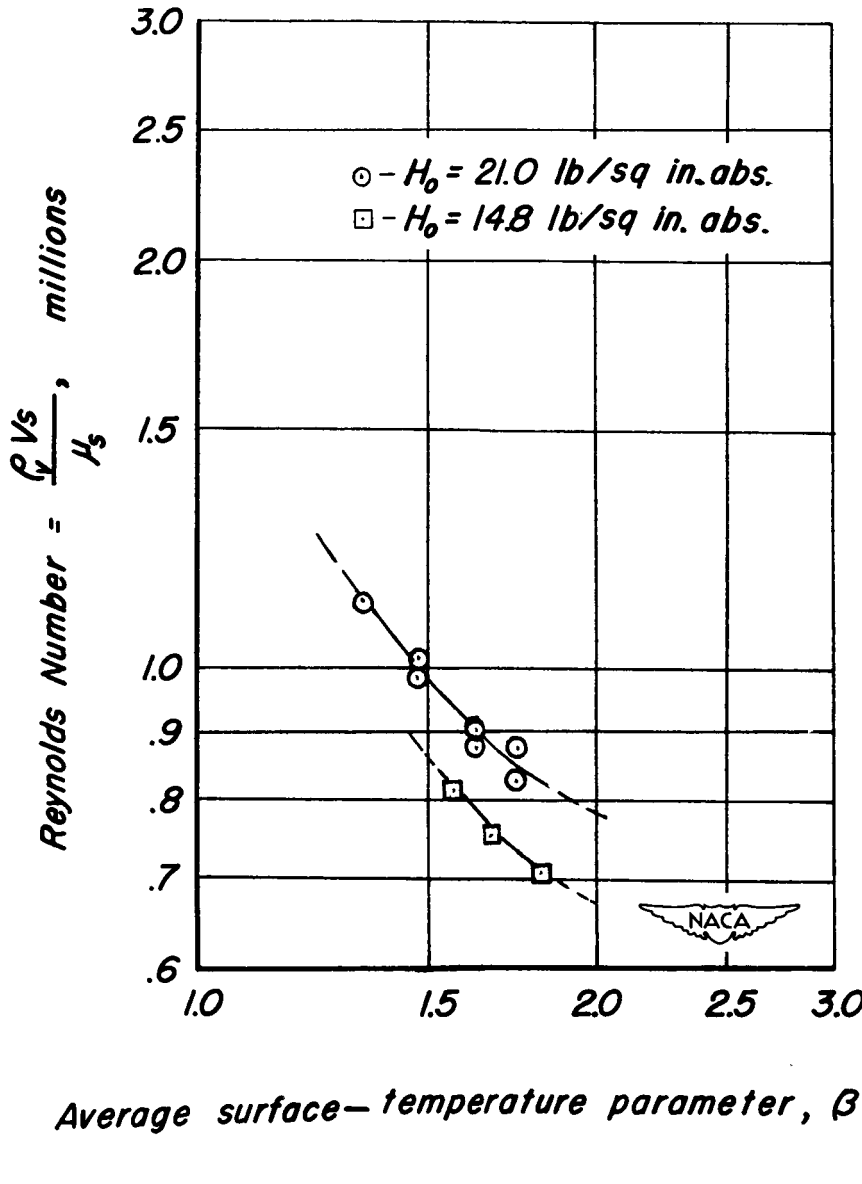

Figure 13. —The variation of the length Reynolds number at transition with surface-temperature parameter on a heated 20° cone.

[redacted]

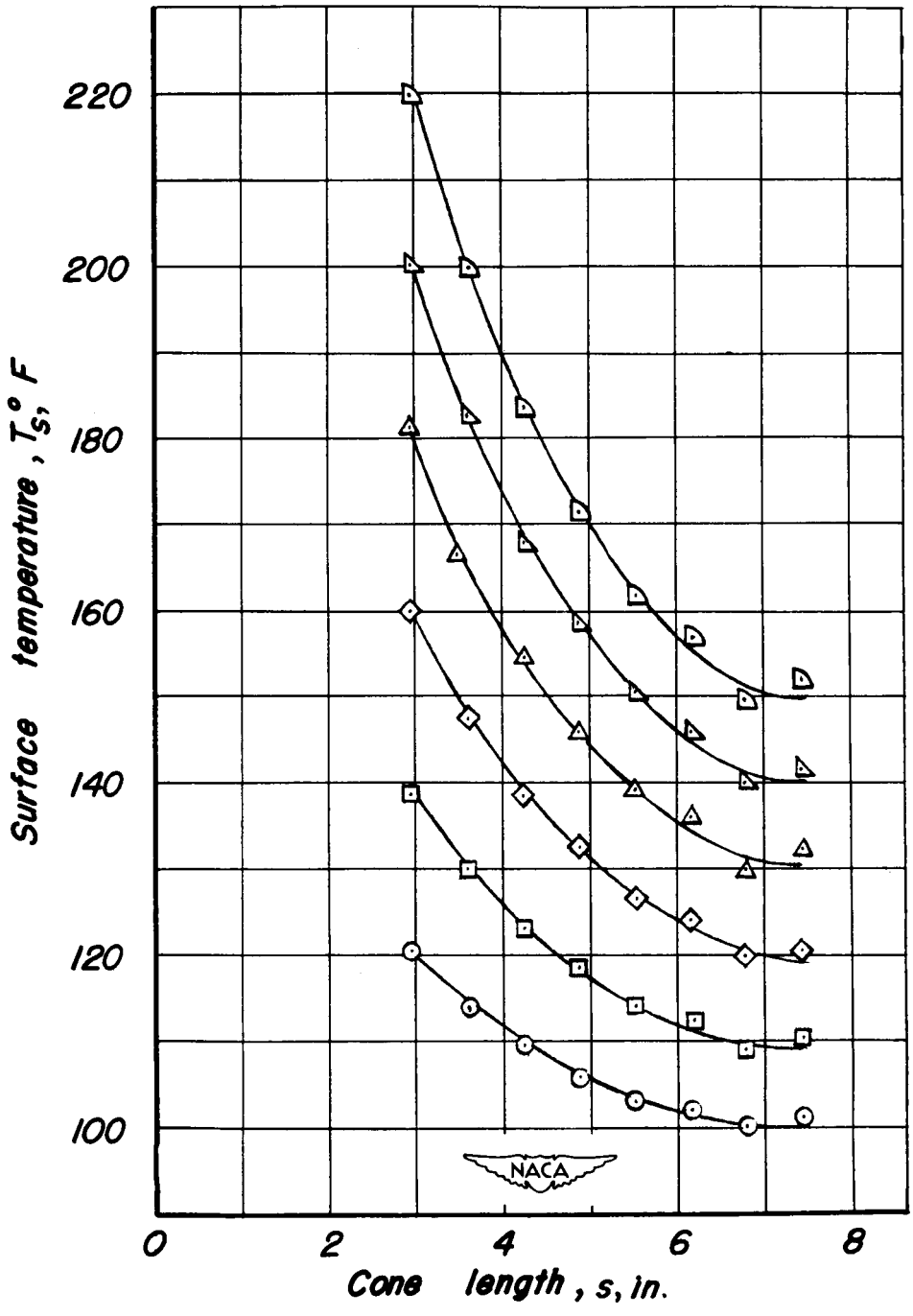

(a) H_0 = 8.7 lb/sq in. abs.

Figure 14.— Surface — temperature distributions for various nominal surface temperatures on the heated 20° cone with a turbulent boundary layer.

[redacted]

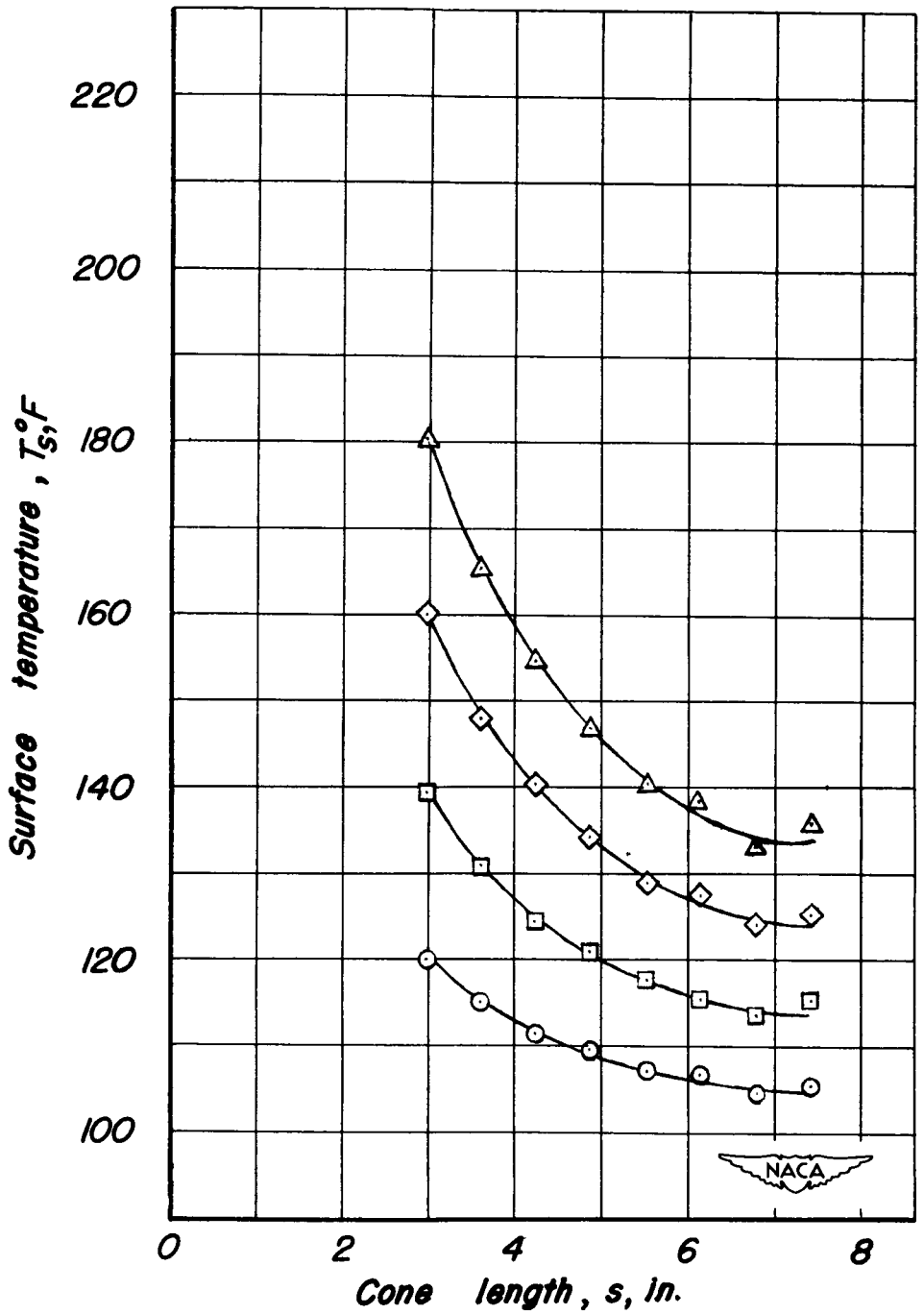

(b) H_0 = 14.8 lb/sq in. abs.

Figure 14.—Concluded.

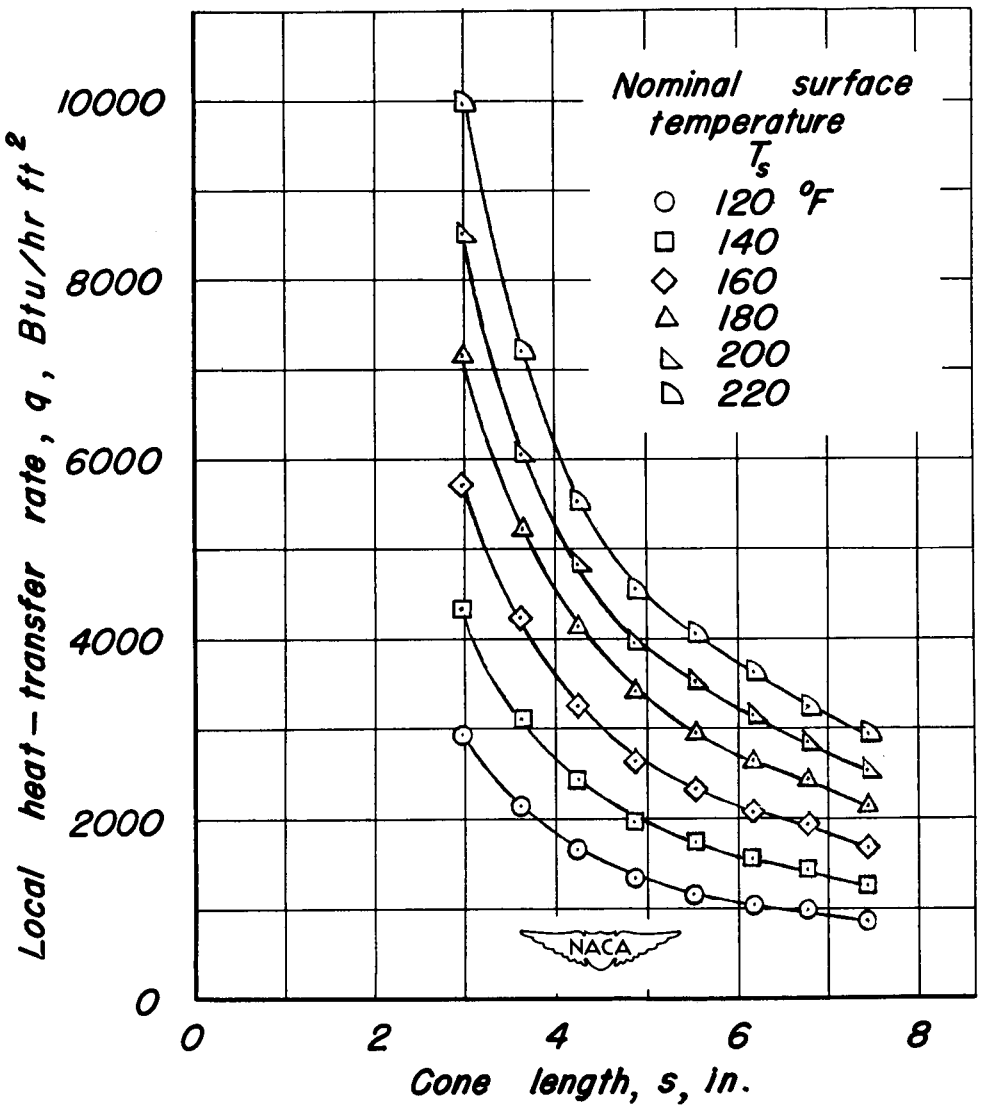

(a) H_0 = 8.7 lb/sq in. abs.

Figure 15.- Distribution of local rate of heat transfer on a 20° cone with a turbulent boundary layer.

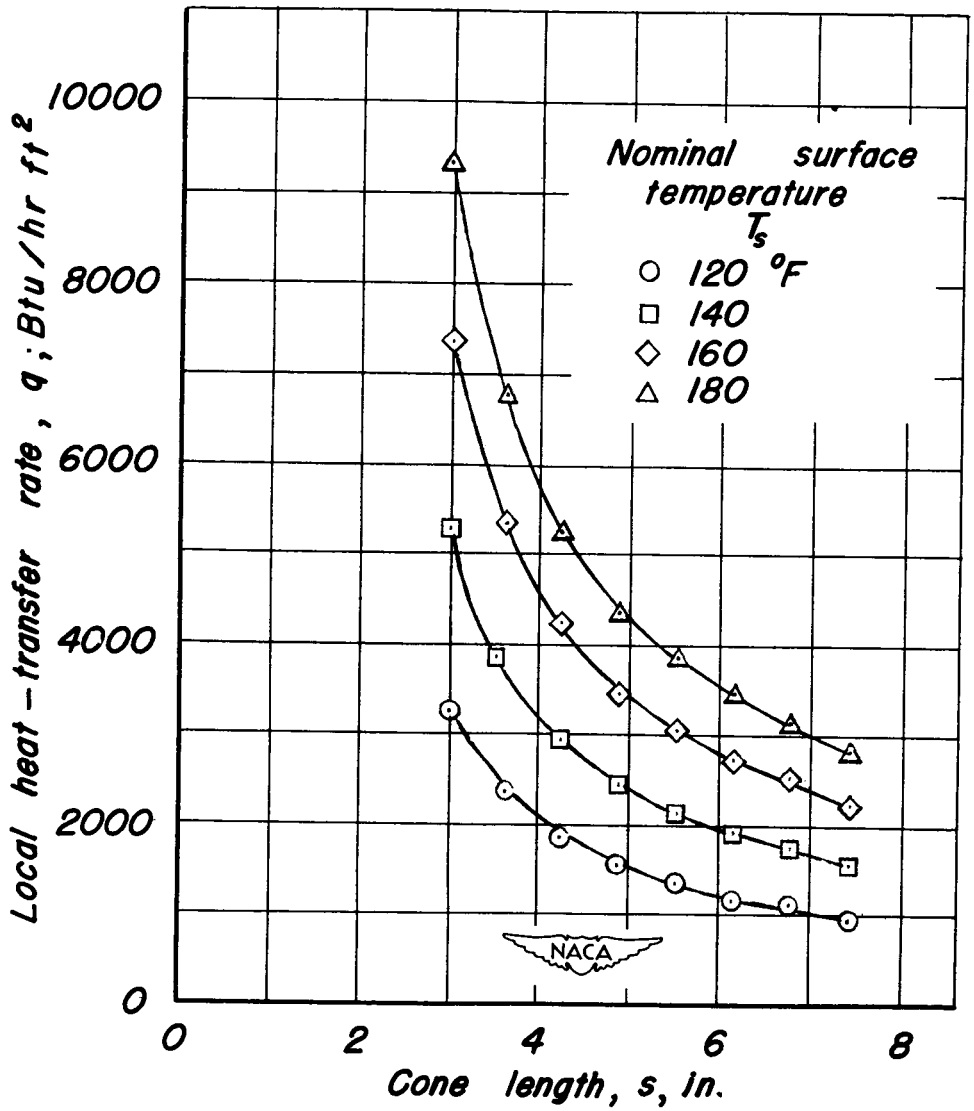

(b) H_0 = 14.8 lb/sq in. abs.

Figure 15.—Concluded.

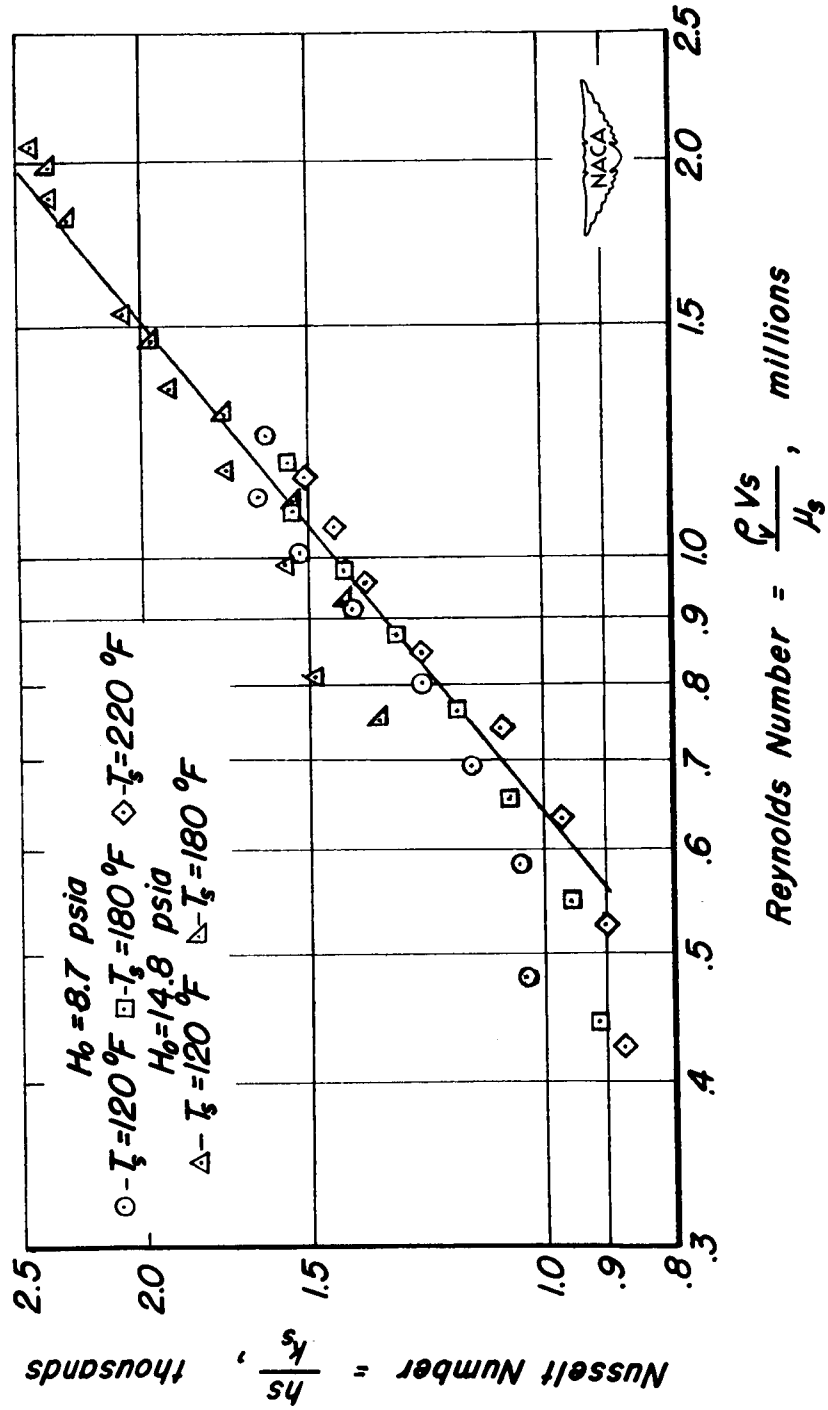

Figure 16. — The variation of local Nusselt number with length Reynolds number on a heated 20° cone with a turbulent boundary layer.

[redacted]

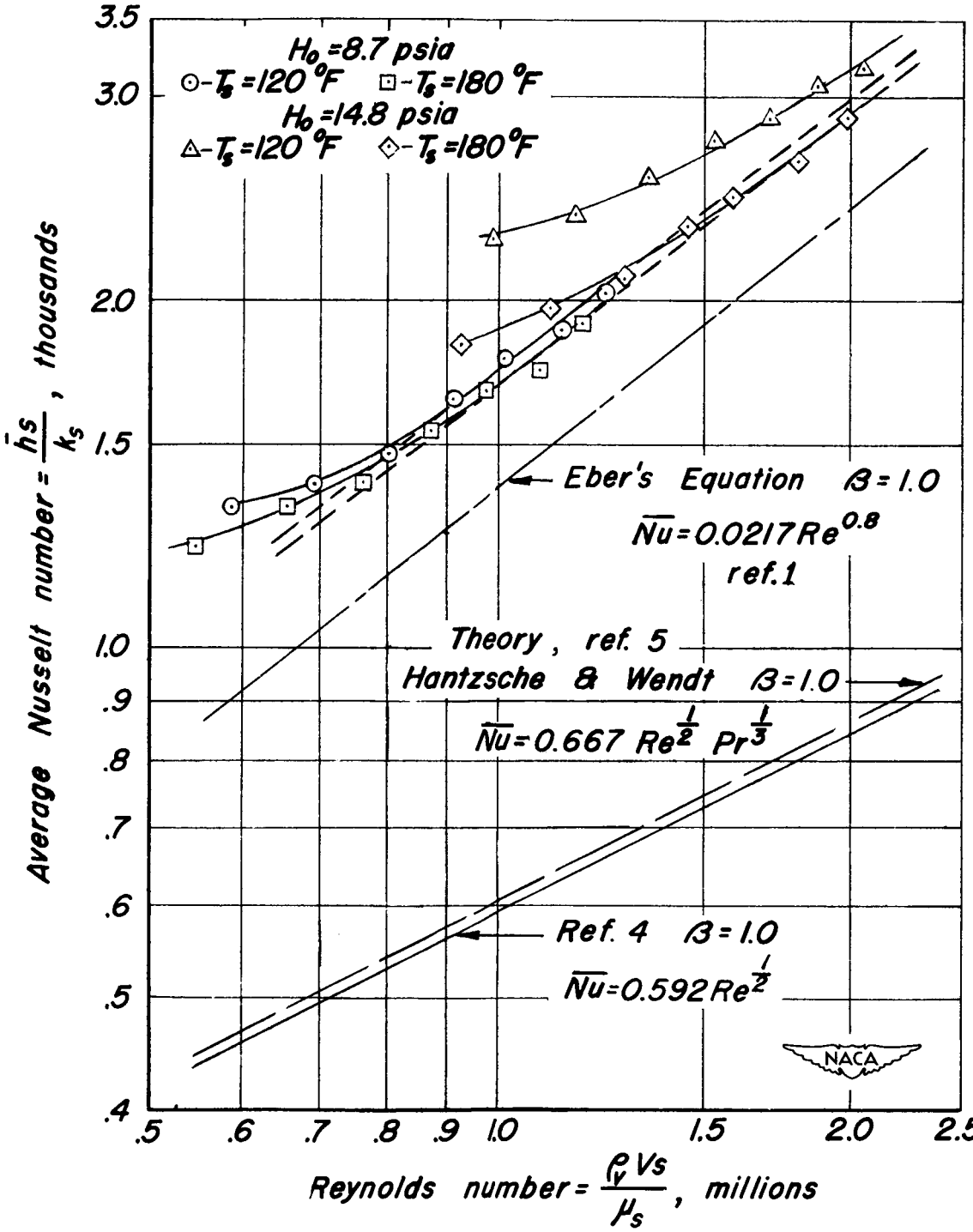

Figure 17. —A comparison of experimental data with Eber's equation and the Hantzsche and Wendt equation for a 20° cone with a turbulent boundary layer.

[redacted]

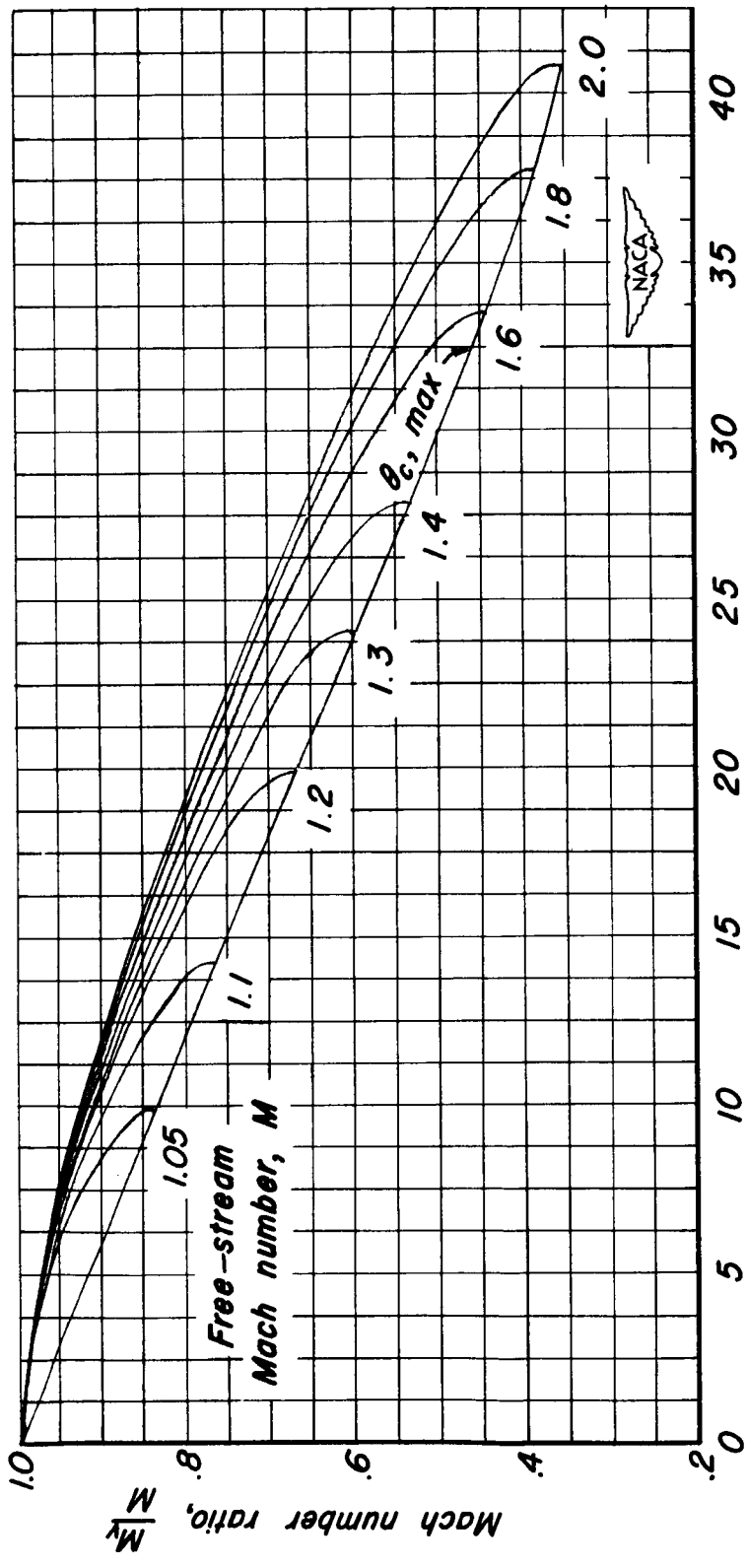

(a) Relation between surface Mach number and cone half-angle for various free-stream Mach numbers (reference 11).

Figure 18.-Design charts.

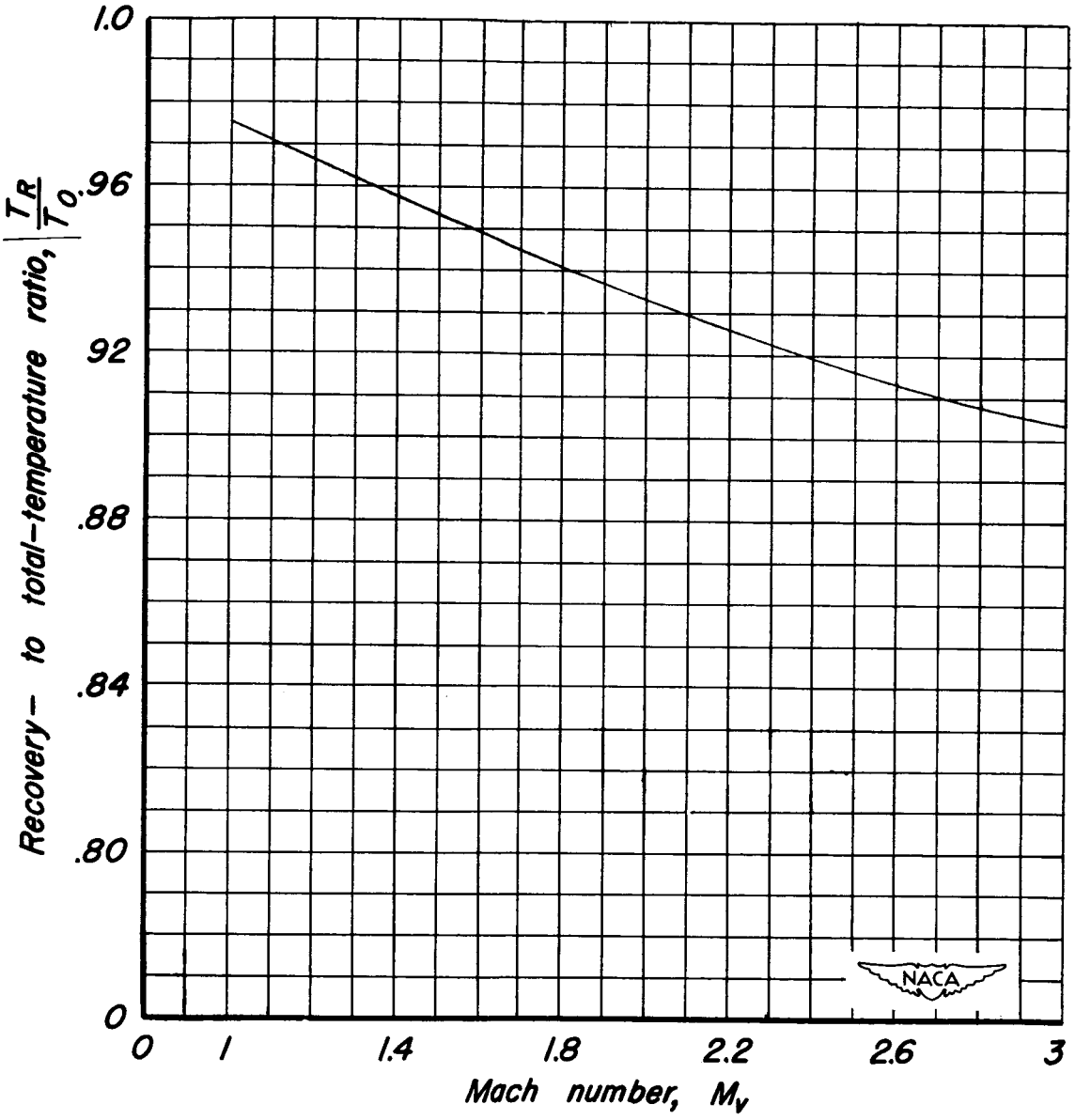

(b) The variation of the ratio of recovery to total temperature with Mach number.

Figure 18.—Continued.

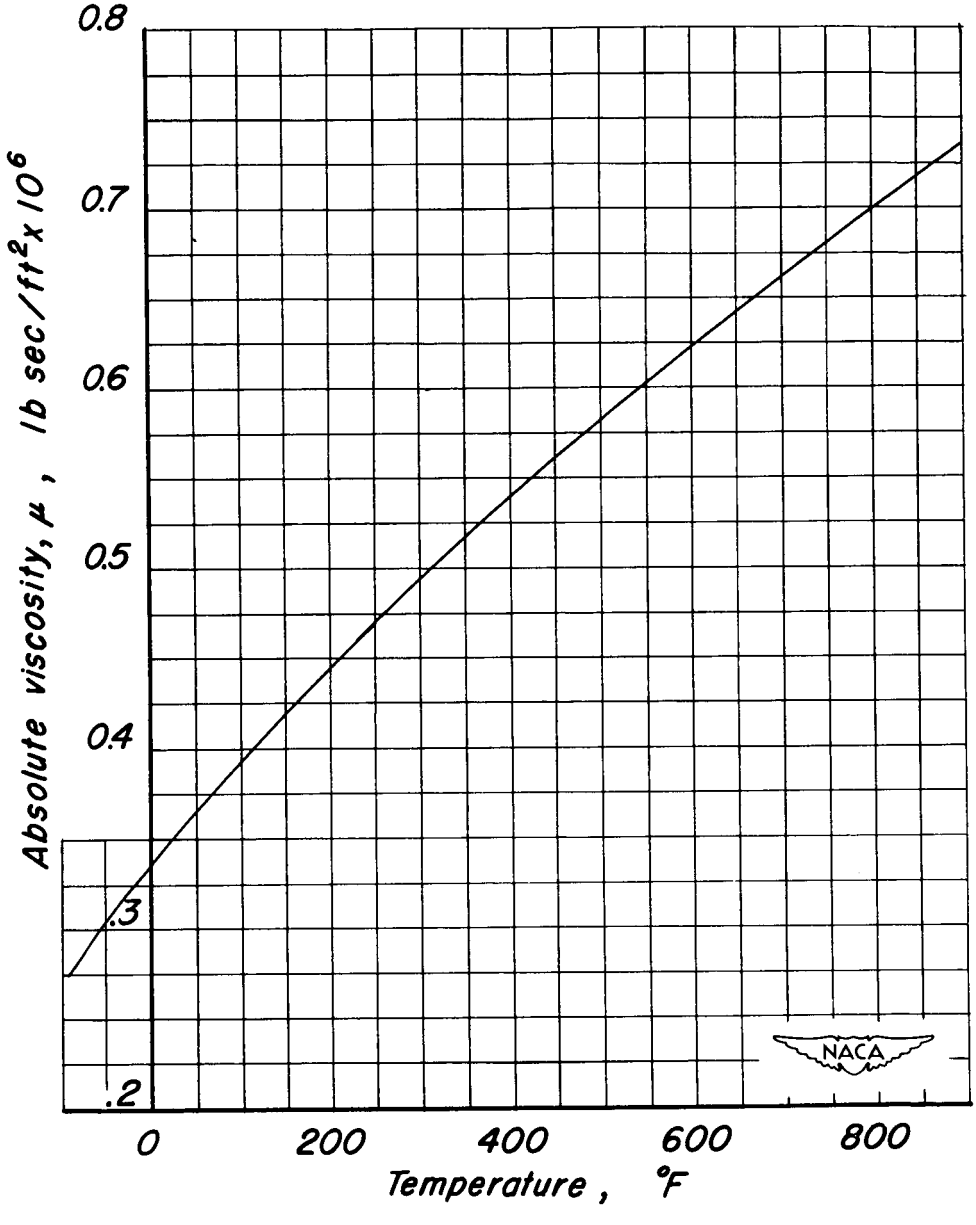

(c) The variation of absolute viscosity of air with temperature.

Figure 18.—Continued.

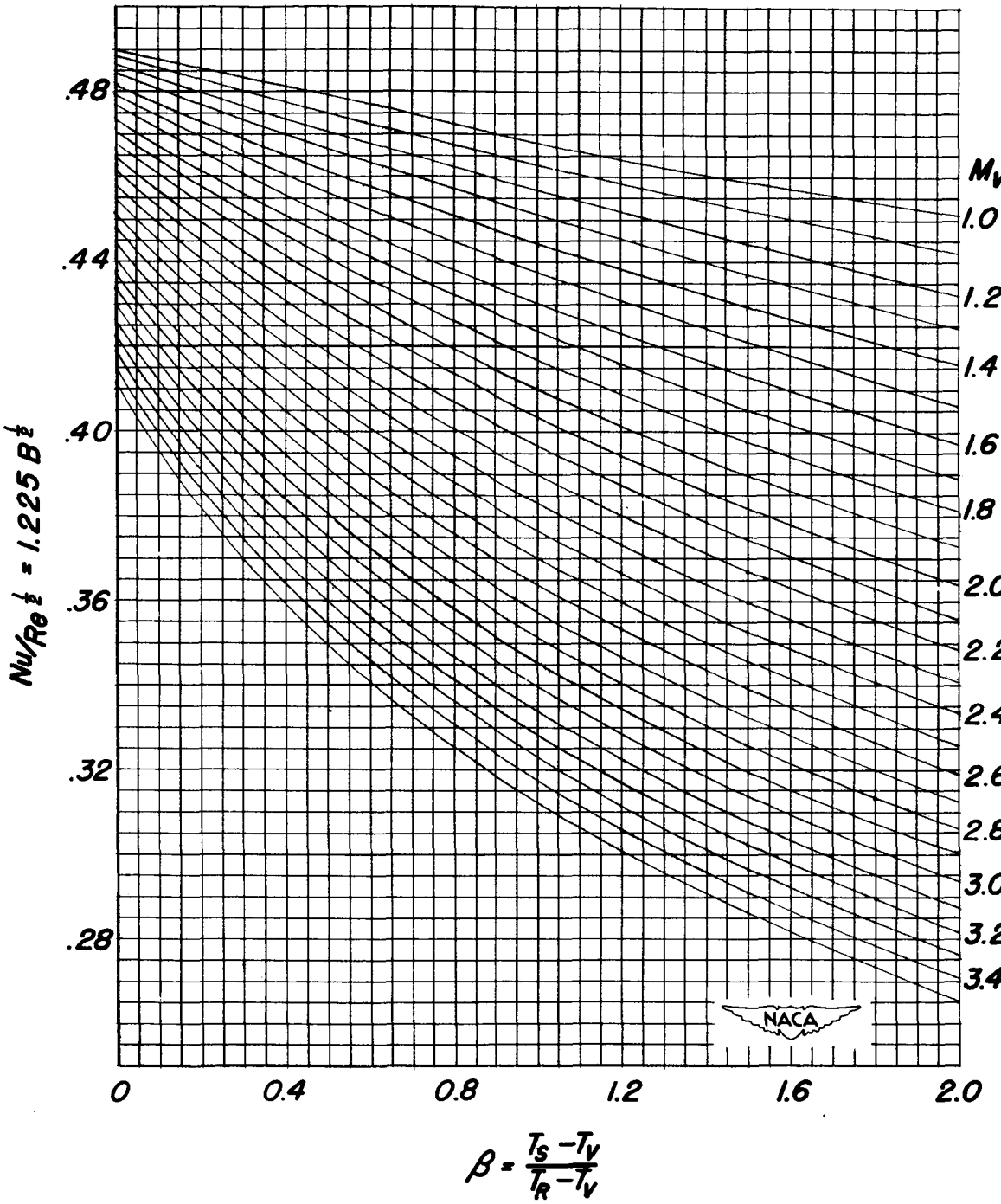

(d) The variation of local Nusselt number with surface-temperature parameter, Mach number, and Reynolds number for cones with laminar boundary layers.

Figure 18. — Continued.

[redacted]

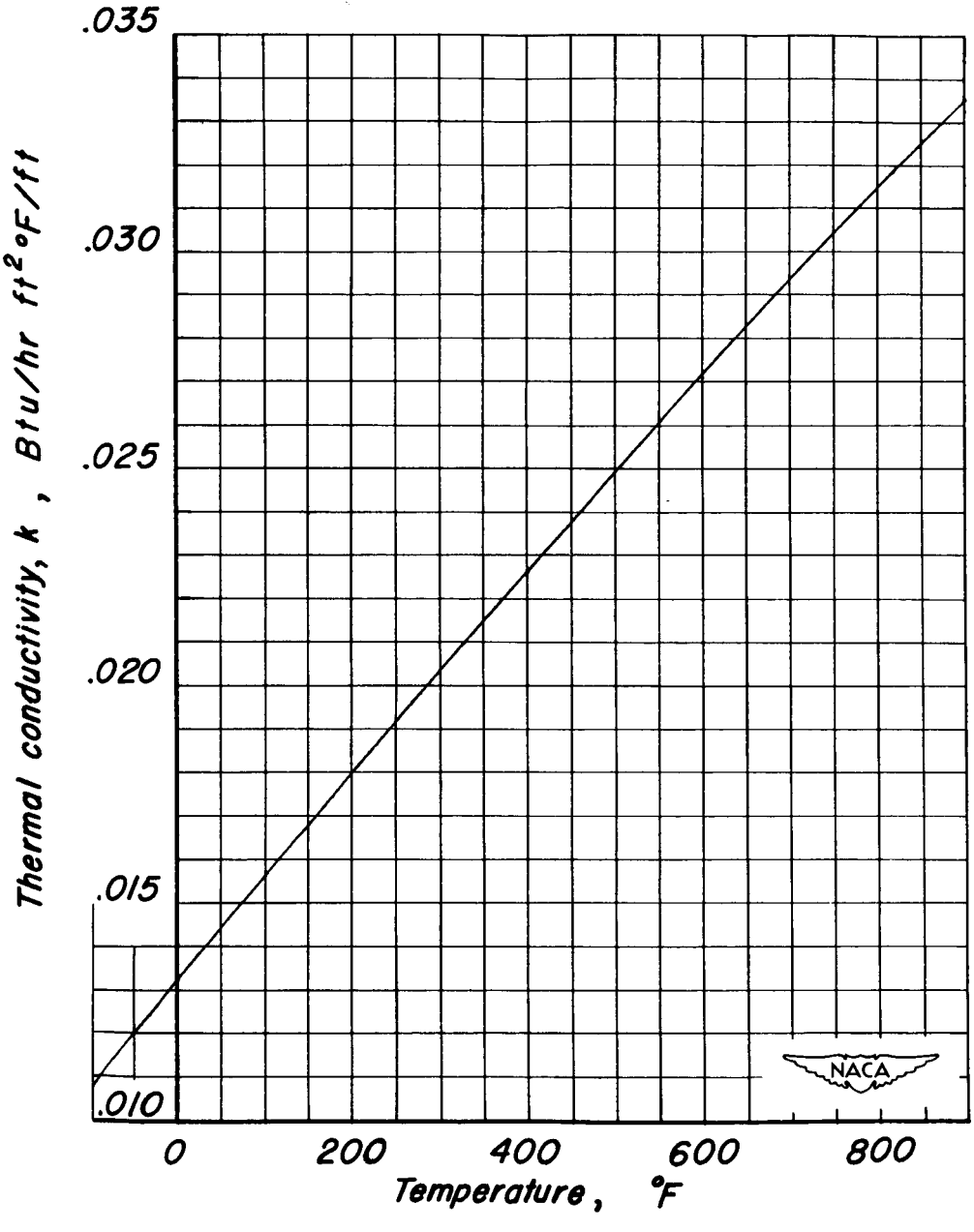

(e) The variation of thermal conductivity of air with temperature.

Figure 18.—Concluded.

[redacted]

E R R A T A

NACA RM No. A8L28

HEAT-TRANSFER AND BOUNDARY-LAYER TRANSITION ON A HEATED 20° CONE AT A MACH NUMBER OF 1.53

By Richard Scherrer, William R. Wimbrow, and Forrest E. Gowen

January 1949

The following changes should be noted:

Figure 17, Eber's equation should be:

$$Nu = 0.0149\ Re^{0.8}$$

instead of

$$Nu = 0.0217\ Re^{0.8}$$

The line in figure 17 indicated as resulting from Eber's equation should be changed to correspond to the change in the equation.

[redacted]

MAY 31 1949